Aircraft noise prediction

A comparison between current established methods

S. M. Haasdijk

Technische Universiteit Delft

TU Delft

Aircraft noise prediction

A comparison between current established methods

by

S. M. Haasdijk

to obtain the degree of Master of Science
at the Delft University of Technology,
to be defended publicly on Friday November 25, 2016.

Student number:	4031571	
Project duration:	April 24, 2016 – November 25, 2016	
Thesis committee:	Prof. dr. D. G. Simons,	TU Delft, Chair Aircraft Noise and Climate Effects
	Dr. M. Snellen,	TU Delft, Supervisor
	Dr. ir. M. Voskuijl,	TU Delft

TU Delft

Abstract

Noise prediction models are critical to the assessment of noise generated by aircraft. The research objective of this MSc research project was to compare the noise predictions of an empirical noise prediction model and a semi-empirical prediction model. Both models were assessed on their use, applicability and their limitations and how these result in the noise predictions. The noise predictions of the Noise Impact Reduction and Optimization System (NIROS), an empirical noise prediction model used by Deutsche Flugsicherung (DFS the German air traffic control), were compared with the noise predictions of the Parametric Aircraft Noise Analysis Module (PANAM). PANAM is a noise prediction model developed by the research institute Deutsches Zentrum für Luft- und Raumfahrt (DLR).

To get a better understanding of the methods used in both models, literature on the subject was consulted. Moreover the documentation of PANAM and NIROS and the source code of NIROS were reviewed. Three major difference were found during this part of the research i.e. the use of Noise-Power-Distance tables in empirical noise modelling and noise source modelling in semi-empirical noise models, the differences in noise propagation methods applied for ground reflection and atmospheric absorption and the differences in the construction of the flight path.

A simulation case was constructed to further examine the differences in the noise predictions of both models. In PANAM and NIROS an A319 was used to simulate the noise for observers located on the ground. The results of the simulations showed higher noise levels in PANAM than in NIROS. The trend of the noise levels at closely spaced observer positions directly underneath the flight path was comparable. In PANAM more variations were visible due to the separate modelling of the noise sources and the type of data used in this model. Some factors which can explain these results were analysed. The difference in flight path and the applied ground reflection method had the biggest influence on the simulation results. Validating the simulations with measurements showed that PANAM seems to overestimate the noise and NIROS underestimate the noise.

Better understanding of the differences can be used to make improvements to the fully empirical method. In this research some improvements were proposed. A possible improvements of NIROS is to include more vertical flight profiles, this will increase the flexibility of the model. Moreover more methods for ground reflection can be implemented to include the effects of different types of soil. Also correction factors for steep thrust increase/decrease and slat and gear extension might improve NIROS.

Although the goal to construct a first comparison between empirical and semi-empirical models was achieved, the conclusions of this research only hold for the noise predictions of the A319. For future work it would be recommended to compare simulations of different aircraft types if more data is available. This will show if there is always an offset present between the predictions of the two types of models. More validation data, and more exact levels, would better support the conclusions. More research will thus make it possible to check if the conclusions of this research are valid in general.

Acknowledgements

It would have been impossible to complete this MSc thesis without the help and support I received from some people. I would like to thank them for their guidance during my thesis work.

First of all I want to thank Mirjam Snellen, my TU Delft supervisor, for her constructive feedback on my research and writing. She helped me to zoom out and stay focussed on the bigger picture of the research. Furthermore I would like to thank Dick Simons, the chair of the Aircraft Noise and Climate Effects section, for creating the opportunity to work in collaboration with DLR and DFS. Moreover I want to thank him for his feedback during several meetings.

The majority of my research was conducted in Germany at the DFS. I would like to thank them for this opportunity. In particular I want to thank Sascha Wichmann for his feedback and help during my stay. Moreover I want to thank Lothar Bertsch of DLR for the support and answering question regarding PANAM.

Last, but not least, I want to thank my family and friends for keeping me positive. Especially I want to thank my father for his enthusiasm and patience to proof-read my entire thesis.

S. M. Haasdijk
Delft, November 2016

Contents

List of acronyms

3D	Three Dimensional
AIP	Aeronautical Information Publication
ANoPP	Aircraft Noise Prediction Program
ANP	Airport Noise and Performance database
ANSI	American National Standards Institute
ANSP	Air Navigation Service Provider
CAS	Calibrated Airspeed
CPA	Closest Point of Approach
DFS	Deutsche Flugsicherung
DLR	Deutsches Zentrum für Luft- und Raumfahrt
EASA	European Aviation Safety Agency
ECAC	European Civil Aviation Conference
EDOP	Schwerin-Parchim airport
EPNL	Effective Perceived Noise Level
FAA	Federal Aviation Administration
Full D	Full Deployment
IATA	International Air Transport Association
ICAO	International Civil Aviation Organization
INM	Integrated Noise Module
LDLP	Low Drag Low Power procedure
MODATA	Modified IATA procedure
NASA	National Aeronautics and Space Administration
NIROS	Noise Impact Reduction and Optimization System
NPD	Noise-Power-Distance
PANAM	Parametric Aircraft Noise Analysis Module

PrADO	Preliminary Aircraft Design and Optimization
RH	Relative Humidity
SAE	Society of Automotive Engineers
SEL	Sound Exposure Level
SPL	Sound Pressure Level
TAS	True Airspeed

List of symbols

Sign	Description	Unit
$\Delta\xi$	Change in heading	$^\circ$
$\Delta\xi_{trans}$	Transition sub arc	–
ε	Bank angle	$^\circ$
λ	Length of the flight path segment	m
δ	Ratio of the ambient air pressure at the aircraft to the standard air pressure at mean sea level	–
γ	Ratio of specific heats	–
ρ	Density	kg/m^3
α	Atmospheric attenuation coefficient	dB/m
β	Elevation angle	$^\circ$
$\Lambda(\beta, l)$	Correction factor lateral attenuation	–
$\varphi(x, y, z)$	Quasi-stationary flight path positions	m
ΔL_A	A-weighting correction	dB
α^*	Emission angle 1 PANAM	$^\circ$
β^*	Emission angle 2 PANAM	$^\circ$
Δ_F	Correction factor finite segments	–
σ_e	Effective flow resistivity	$^\circ$
Δ_v	Correction factor duration	–
$\Delta i(\varphi)$	Correction factor engine installation effects	–
Δs	Horizontal track distance	m
A_a	Transmission loss due to atmospheric absorption	dB
D	Flap coefficient	$kt/\sqrt{lbf}$
F_n	Net thrust per engine	lbf
F_n/δ	Corrected net thrust	lbf
I	Acoustic intensity	W/m^2

Sign	Description	Unit
L_A	A-weighted sound level	dBA
$L_{A_{max}}$	Maximum A-weighted sound level	dBA
P	Power setting	–
R	Radius	m
T	Temperature	$^{\circ}C$
V	Velocity	m/s
W	Weight	lb
d	Observer distance	ft
g	Gravitational acceleration	ft/s^2
l	Lateral displacement from the ground track	m
p	Pressure	Pa
p_e	Effective sound pressure	N/m^2
p_{e_0}	Reference effective sound pressure	N/m^2
q	Distance between the end point of the segment and the point closest to the observer perpendicular to the segment	m
r	Turn radius	ft
r	Propagation distance	m
s_{TOG}	Take off ground roll length	m
t	Time	s
x	x Coordinate	m
y	y Coordinate	m
z	Height	m

1 Introduction

Due to the increasing population and the growing air transport the prediction of aircraft noise becomes more important. Aircraft noise can cause community annoyance, complaints and in very severe cases hearing loss. Several regulations and laws are introduced to reduce the noise pollution. Noise prediction models are critical to the assessment of noise generated by aircraft. Three types of noise prediction models are currently used to assess the noise influence; empirical noise prediction models, semi-empirical noise prediction models and fully numerical models. The first two are widely used and will be considered in this research.

The subject of this research is the investigation of the differences between two aircraft noise prediction models. The two types of models are used by separate stakeholders. Empirical models are often used by Air Navigation Service Providers (ANSPs) and semi-empirical models are more used by research institutes. No direct comparisons are documented in literature known to the author and this will be valuable for the improvement of noise prediction models. One fully empirical model and a semi-empirical model are used in this research. The noise predictions of the Noise Impact Reduction and Optimization System (NIROS), an empirical noise prediction model used by Deutsche Flugsicherung (DFS the German air traffic control), will be compared with the noise predictions of the Parametric Aircraft Noise Analysis Module (PANAM). PANAM is a noise prediction model developed by the research institute Deutsches Zentrum für Luft- und Raumfahrt (DLR).

1.1. Current state of research

Empirical models such as NIROS are used to predict aircraft noise of multiple approaches and landings. This to calculate the influence of the presence of an airport on the community. Semi-empirical models are more used by research institutes to predict the influence of a new aircraft configuration or flight procedure on the produced and received noise. It is useful to compare these two types of models to learn more about their use and applicability.

No direct comparison of these models is described in any research paper. Some papers [26][33] describe the comparison between models. But these all compare models of the same category.

Filippone and Bertsch [26] compared the two semi-empirical models FLIGHT and PANAM. Also a comparison of these models with measurement data was made. FLIGHT is a commercial software framework developed for the performance prediction of commercial gas turbine aircraft. This program also contains a module which predicts the noise using the method of components i.e. separate modelling of all noise sources. Filippone and Bertsch described the accuracy of the noise models implemented in PANAM and concluded that the airframe noise source models and propulsion noise source models have an accuracy of ± 1 dB(A) and ± 4 dB(A) respectively. An uncertainty in PANAM is the data input. Vehicle parameters which are not provided by the manufacturer are estimated with the simulation model Preliminary Aircraft Design and Optimization (PrADO). Simulations of airframe noise and engine noise of an A319-100 directly below the flight path were compared using both models. The overall noise predictions were compared with measurement data of the Parchim 2006 [43] measurement campaign. Discrepancies of the models PANAM and FLIGHT were mainly present when the high lift devices and/or landing gear were deployed. These differences can be attributed to the time differences between both simulations when deploying the high lift devices. This has a major influence on the predicted noise.

Isermann and Vogelsang [33] compared the two fully empirical methods AzB [17] and ECAC Doc.29 [14][15] (the guideline of NIROS). This comparison is not supported with data. It only describes the methods applied and the assumptions made in both methods. They concluded that the acoustic model of AzB is more flexible due to the explicit modelling of directivity. Doc. 29 implementations are better adjustable for modelling flight operations. Moreover Doc. 29 models are based on the Airport Noise and Performance (ANP) database and might be better suitable for an international fleet.

Thus in current research, noise prediction models are compared code-to-code or with the use of measurement data. However, at this moment in time, no comparison is documented between an empirical noise prediction model and a semi-empirical noise prediction model.

1.2. Research objective and goals

The research objective of this MSc research project is to compare the noise predictions of an empirical noise prediction model and a semi-empirical prediction model. Both models will be assessed on their use, applicability and their limitations and how these result in the noise predictions.

The models used are the empirical noise prediction model NIROS and the more physics based model PANAM. The end goal of this research is to investigate to what extent the predictions by the models are in agreement. Better understanding of the differences might be used to make improvements, especially to the fully empirical method.
Two research questions were formulated to support the research objective and goals. These research questions are:

1. What are the major differences between empirical noise prediction and semi-empirical noise prediction models when predicting aircraft noise?

2. What are possible improvements of the empirical noise model NIROS based on the comparison with the more physics-based model PANAM?

These research questions will be answered using a case study of PANAM and NIROS. This research will be highly relevant for the improvement of noise prediction models. At this moment in time the two types of aircraft noise prediction models are used by two separate stakeholders i.e. research institutes and air navigation services of air traffic control. No comparison is documented and this will be valuable in order to improve the models. Moreover this research will also assess the applicability of semi-empirical models for practical purposes. The results might directly contribute to the improvement of the model NIROS used at DFS.

1.3. Research structure

In this report first a literature review is presented in chapter 2. The initial step in this research is to compare the two model methodologies using their manual and source code. This will give a good impression of the used methodologies in both models. The detailed model assessment of NIROS and PANAM is described in chapter 3. After this a simulation will be executed in both models. This will give an indication of the differences in predictions of both models. The simulation set-up and results are presented in chapter 4. The results of the simulations will be further analysed in chapter 5. The results are validated with measurement data in chapter 6. This chapter will also discuss the key differences between the models. In chapter 7 a small sensitivity analysis is presented which will be used to answer the second research question. In chapter 8 the conclusions of this research are stated and recommendation for future work are given. The structure of this report is shown in figure 1.1.

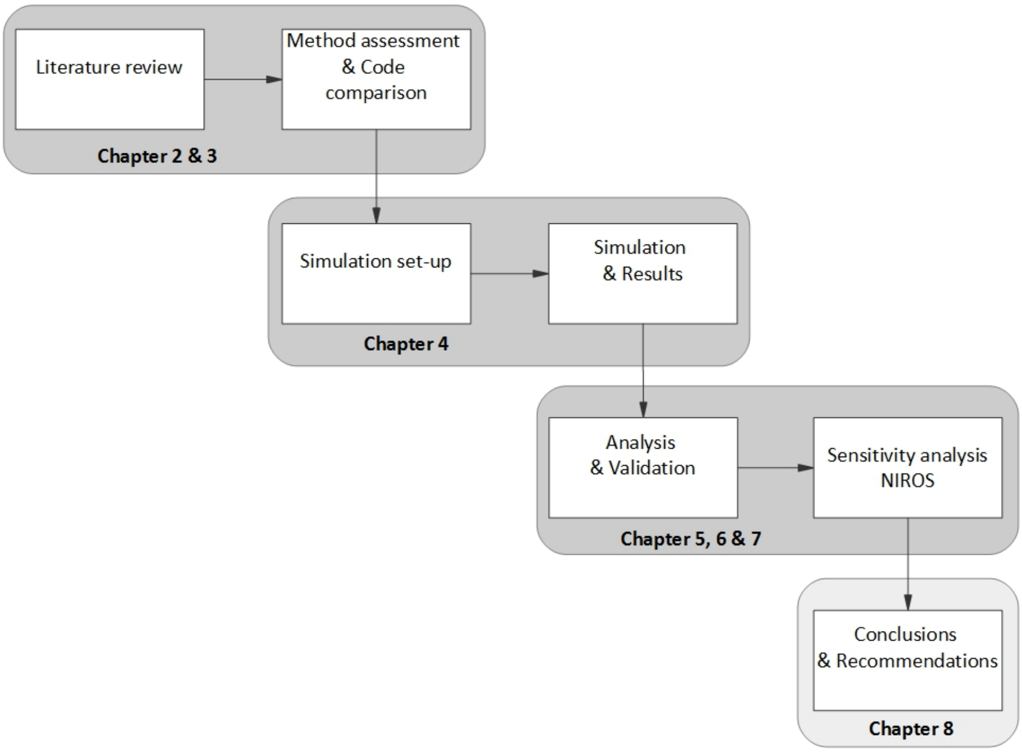

Figure 1.1: Research structure

2
Literature review

Theoretical research on noise prediction started in the early 70s. One of the first physics based computer code for overall noise prediction was created by the Federal Aviation Administration (FAA) together with the National Aeronautics and Space Administration (NASA) and was called Aircraft Noise Prediction Program (ANoPP). In this model, individual noise sources were modelled separately and the model also calculated the propagation through the atmosphere. Around the same time best practise models were developed for civil aviation, who required a fast and practical model. The Integrated Noise Module (INM) is an example of such a model.[25] The first version of this model, used by the air traffic management, made use of empirical data and was based on the use of Closest Point of Approach (CPA). In this type of model the noise impact at the point of immission is calculated from the noise level of the shortest distance to the flight path.[36] The data was collected by measurements of flyovers, summarised in so-called Noise-Power-Distance (NPD) tables. A good example of such a model is the German method AzB which was published in 1975. The model is simple and requires short computing times. However, the model proved to be simplified too much, not meeting the required accuracy.[10] Later on, a more advanced method of the implementation of the flight path in noise modelling was introduced. With this, curved flight paths and different thrust settings could be modelled more accurately.[36]

Currently the 'method of components', individually modelling of noise sources and combining these, is still the method used by research institutes for noise prediction simulations. In this method the noise sources of an aircraft are all modelled independently. A good example of this approach is adopted in the model ANoPP and its successor ANoPP2. Air traffic control often uses models based on NPD tables or other measurements.

In this research the aircraft noise prediction models are divided in fully data-based empirical models and semi-empirical more physics based models. The first category consists of models which are fully based on measurement data and thus empirical. The semi-empirical category consist of simulation models which are based on empirical noise source models combined with noise propagation models.

In section 2.1 some background information regarding aircraft noise sources is given, followed by the outline of empirical models in section 2.2. The semi-empirical noise prediction models are described in section 2.3.

2.1. Aircraft noise sources

In literature the aircraft noise sources are roughly divided in airframe noise and propulsion noise [25] [8]. Airframe noise consists of sound produced by the wing, landing gear and high lift devices. In the past the propulsion system was the primary source of aircraft noise [49]. However, due to the introduction of more silent engines, airframe noise became more comparable to propulsive noise. This section will describe the two main noise sources. Finally, installation effects will be discussed briefly.

2.1.1. Airframe noise

Due to the modern silent engines, airframe noise is of comparable magnitude as propulsion noise. Airframe noise can be dominating nowadays during the approach due to the deployment of landing gear and high lift devices. The main contributors to airframe noise are the landing gear, slotted slats, flap and slat side edges, flap and slat tracks, spoilers and component interaction noise sources.[18] Turbulent flow over these components causes broadband noise. In figure 2.1 all airframe noise sources are shown.

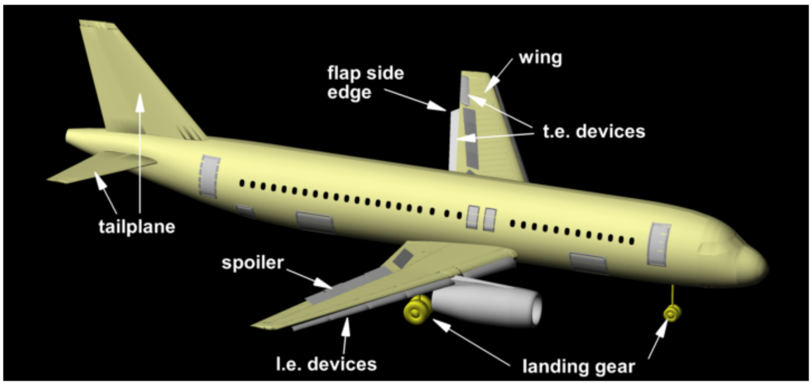

Figure 2.1: Airframe noise sources [8]

Casalino et al. [13] describe in detail the main mechanisms of airframe noise:

- Wing; trailing-edge scattering of boundary-layer turbulent kinetic energy into acoustic energy
- Slat; the vortex shedding from slat/main-body trailing-edges, the possible gap tone excitation through non-linear coupling in the slat/flap coves and the flow unsteadiness in the recirculation bubble behind the slat leading-edge
- Flap; the roll-up vortex at the flap side edge
- Landing gear; multi-scale vortex dynamics and the consequent multi-frequency unsteady force applied to the gear components

2.1.2. Propulsion noise

There are multiple types of aircraft engines. However currently turbofan and turbojet engines are the most common propulsion systems. These are thus the type of engines considered in this section. For these engine types, various propulsion noise sources can be identified [49][2][8]:

1. Jet
2. Fan
3. Turbine
4. Core; consisting of combustion and compressor noise

These sources are shown in figure 2.2.

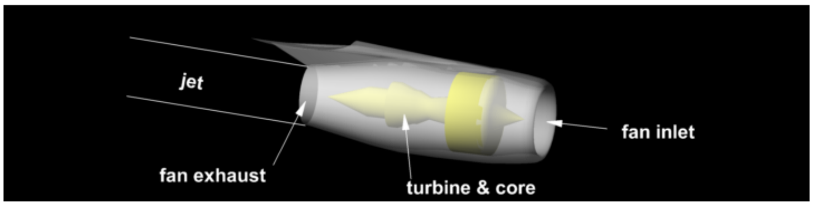

Figure 2.2: Propulsion noise sources [8]

Jet noise is also called jet mixing noise and is generated by the turbulence in the jet flow. At the exhaust nozzle of the engine high velocity exhaust is mixed with ambient air. Lighthill [38] was the first to describe the acoustic analogy. In the power law he described the acoustic intensity of a jet to be proportional to the exhaust velocity to the 8th power [53] as:

$$I \propto v^8 \tag{2.1}$$

This analogy holds for cold jets. Hot jets are generally quieter than cold jets.[9] Fan noise consists of both broadband and tonal noise. For subsonic aircraft tonal noise is dominating. At the eigenfrequency of the fan blade and the higher harmonics the noise level is the highest. This is also called 'fan whine'.[49] The broadband noise is caused by flow turbulence or vortex shedding. So-called 'buzz-saw' noise is generated when supersonic flow collides with the fan resulting in shock waves. This noise is tonal and appears during take-off and climb.[41]

Combustion noise is generated during the combustion of the fuel. The gas expands and interacts with its surroundings producing sound waves.[2] This type of propulsion noise has a low frequency (peak levels around 400-500 Hz). Both compressor noise and turbine noise are predicted to be of low magnitude in comparison with jet and fan noise.[3] However the attention for this field of research is growing. Core noise is of growing importance when it comes to noise reduction technologies.[31]

2.1.3. Installation effects

Installations effects have influence on the perceived noise on the ground. The sound is changed due to the interference with other components or due to the aircraft geometry. Well-known installation effects are the interaction of engine sound with the surface of the wing or the effect of the flap-landing gear interaction. [28] [51]

2.2. Empirical noise prediction models

The main building blocks of empirical models are the databases with noise- and performance data and the approximations of the flight path. These two are used to predict the aircraft noise at an observer location. This process can be done for many different observer locations resulting in a so-called noise contour. These kind of models are often used for the prediction of noise around airports.

2.2.1. Noise-Power-Distance (NPD) databases

NPD tables are the most simple and often used databases for fully empirical models. NPD data give the (A-weighted) noise level as a function of distance between the observer and the noise source for a certain set of atmospheric conditions (reference conditions). In these data sets the power setting is also specified.[49] The data originates from flyover measurements, mostly those performed during the aircraft certification. During this certification microphones are placed along the flight track, as shown in figure 2.3. This data includes propagation effects such as atmospheric absorption, spherical spreading and ground reflection.

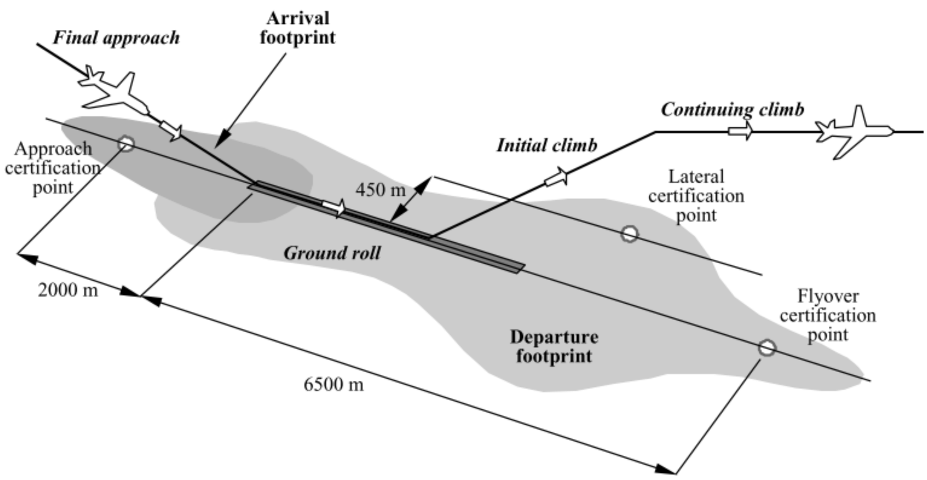

Figure 2.3: Certification measurement points [14]

A disadvantage of using NPD tables is that these are only valid for a specific air absorption and microphone height. Moreover, the separate noise sources in this data cannot be distinguished. Thus the variation in dominant noise sources during different flight procedures is only accounted for in an implicit manner.[25]

The largest NPD database is composed by the FAA and is used in the INM model. In this database the NPD data is normalised to an aircraft speed of 160 knots.[11] A part of this data is also available in the Eurocontrol database 'Airport Noise and Performance' (ANP).

There are also models which rely on their own measurement data, like FLULA2. This data was gathered at Zurich airport with microphones placed at the side and on the centre line of the runway [36]. Together with the radar information of the flight path 1/3 octave noise spectra were obtained [47]. This database consists of directivity characteristics defined as a function of observer distance and longitudinal angle.[14]

2.2.2. Flight path segmentation

Most empirical models make use of flight path segmentation. The flight path is divided in straight segments, and for each segment a noise level is estimated with the use of NPD tables or another database. Sometimes propagation effects are already included, for instance in the NPD tables, otherwise a separate propagation model is needed.

For the vertical flight path (the flight profile) there are two implementations in empirical models: fixed or procedural flight profiles. The fixed method is based on straight segments and a predefined vertical profile. Procedural flight profiles make use of the operating procedure. These procedural steps are used to build up the profile. [33]

2.3. Semi-empirical noise prediction models

In semi-empirical models a more physics-based method of noise prediction is used than in empirical models. The noise is predicted using the method of components. The sources of noise are thus predicted separately. Most models are based on source models described in the 70's. However, improved versions of these source models are used. The semi-empirical models are developed to predict the noise of newer aircraft configurations or flight procedures accurately. The source prediction models for this type of model are described in this section.

2.3.1. Propulsion noise prediction

Most methods for propulsion noise prediction are semi-empirical. Analytical methods exist, but these are only applied for simple problems.

Stone [52] described in 1974 one of the first models for jet noise. This model is based on the acoustic analogy of Lighthill and is improved after 1979 with the effect of forward flight and noise reducing chevrons.[2] Most of the noise prediction models are based on the acoustic analogy of Lighthill or Lilley [39]. Tam and Auriault [54] also developed a semi-empirical model to predict turbulent mixing jet noise. This method is based on the explicitly modelling of sound sources. The propagation in this model is simulated with linearised Euler equations. It was concluded by Morris and Farassat [42] that this model better fits experimental data than the one based on the acoustic analogy. However this is only due to different assumptions. If the same assumptions are made the models are of comparable accuracy.[42]

Heidmann [30] developed a semi-empirical model for fan noise and compressor noise prediction in 1979. This model was updated by Kontos et al. [35] in 1996 to account for newer engines and the use of acoustic lining.[2] For fan noise also analytical (based on the acoustic analogy) and CFD methods exists, but these methods are very computational intensive. Examples of respectively an analytical and computational noise fan models are RSI and LINFLUX, both developed by NASA.[23]

2.3.2. Airframe noise prediction

Fink [27] described in 1977 the first semi-empirical model for airframe noise prediction. In this model all airframe noise sources were calculated separately and it was assumed that they do not have an influence on each other. Fink described the noise from the clean wing, tail, (nose)landing gear, trailing edge flaps and leading edge slats based on measured flyover spectra. There is some critic on the base of this model since the data used is outdated and sparse [25]. However this model is currently used in most of the noise prediction models.

Besides the model of Fink, several other models for airframe noise have been developed. An example of a semi-empirical model used in airframe noise prediction is the model of Guo, Yamato and Stoker[29] for high lift device noise. This model is component-based and makes use of a database with airframe noise data from different aircraft under several flight conditions.[24] Guo also described the most recent landing gear noise prediction model. He compared his model with data from wind tunnel experiments and flight test data. For the prediction of the noise of high lift devices manufactures often develop their own code. However due to the lack of public information these codes cannot be considered in this section.

3

Detailed model assessment of NIROS and PANAM

The purpose of this chapter is to give an overview of the methods used in the noise prediction models NIROS and PANAM. They are assumed to represent the fully empirical and semi-empirical approaches respectively. These models will be used to identify the differences between empirical noise prediction and semi-empirical noise prediction. This model assessment will identify the key differences between the models. In section 3.1 the empirical noise model NIROS will be described in detail. The semi-empirical model PANAM is discussed in section 3.2. Finally, in section 3.3, the most important differences are described.

3.1. NIROS

The Noise Impact Reduction and Optimization System (NIROS) model is based on the ECAC document 29, 3rd Edition (2005) [14] [15]. This document describes a standardized method for aircraft noise contour modelling recommended by the European Civil Aviation Conference (ECAC). The method is based on segmentation and uses a large NPD database with aircraft noise and performance data. The purpose of NIROS is to assess the noise influence of multiple landings and departures. NIROS is used by the DFS to make predictions over a longer time period (days to a year) around airports. The main goal of this model is to identify the best flight procedures from a noise perspective, in order to reduce the impact on the local community. NIROS uses data from the international Aircraft Noise and Performance database (ANP). This is an online database with NPD tables. In figure 3.1 an example of a NPD table is given.

NPD Identifier	Noise Descriptor	Op Mode	Power Setting	L_200ft	L_400ft	L_630ft	L_1000ft	L_2000ft	L_4000ft	L_6300ft	L_10000ft	L_16000ft	L_25000ft
V2527A	SEL	A	2000	93.1	89.1	86.1	82.9	77.7	71.7	67.1	61.9	55.8	49.2
V2527A	SEL	A	2700	93.3	89.2	86.2	83.0	77.7	71.8	67.2	62.0	55.8	49.3
V2527A	SEL	A	6000	94.7	90.5	87.4	83.9	78.5	72.3	67.7	62.5	56.3	49.7
V2527A	SEL	D	10000	95.4	90.7	87.3	83.5	77.7	71.1	66.3	60.9	54.6	47.4
V2527A	SEL	D	14000	100.4	96.1	93.0	89.4	83.5	77.0	72.2	66.7	60.1	53.0
V2527A	SEL	D	18000	103.2	99.1	96.2	92.9	87.4	81.1	76.5	71.1	64.9	57.9
V2527A	SEL	D	22500	105.1	101.2	98.5	95.4	90.3	84.3	79.9	74.8	68.7	62.0

Figure 3.1: Example of a NPD table [15]

The noise is predicted with use of this type of tables. So the distance to the observer (in this case described in ft) and the power setting needs to be calculated within NIROS in order to predict the noise.

In figure 3.2 the layout of NIROS is given. It can be seen that besides the ANP database several other inputs are needed for the prediction of aircraft noise in NIROS. All required inputs of NIROS are shown in table 3.1. The airport and calculation input needs to be provided by the user. These inputs include the ground track of the flight path and the type of aircraft modelled. When modelling multiple aircraft lateral dispersion can be applied. This means that the ground tracks are distributed using a Gaussian normal distributions. This is done to account for deviations in the ground track flown by the aircraft. The ANP database does also incorporates information regarding the aircraft and approach and departure profiles. This information is used in NIROS to construct the vertical flight profile and to calculate the power setting of the aircraft and the distance to the observer. This is all needed in order to predict the noise using the NPD tables.

Population data and topographical data can be included in NIROS. The population data is used to assess the effect of the noise on the community. Topographical data is important when the airport is in the vicinity of mountains or high hills. This affects the received sound for observers on the ground. However it is not mandatory to include this data; without the data NIROS will assume a flat ground surface.

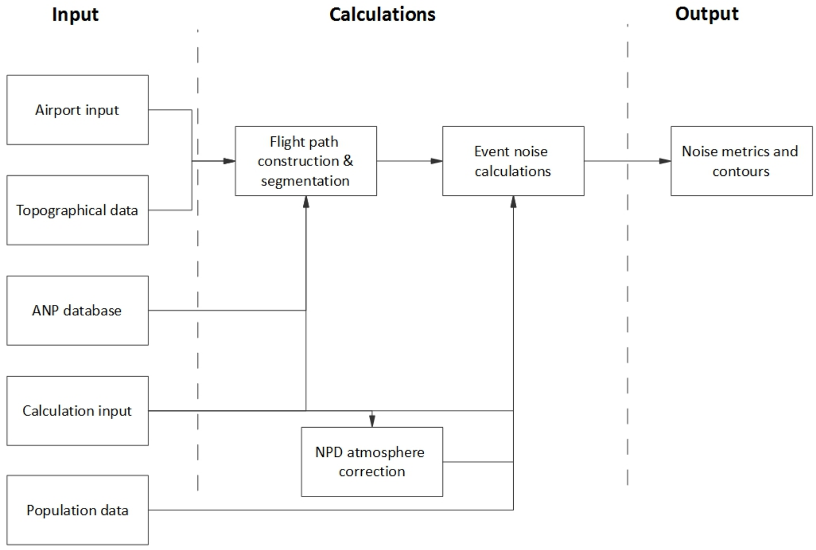

Figure 3.2: Simplified NIROS model flowchart

Table 3.1: Inputs NIROS

Airport input	**ANP database**
Location information	Aircraft data
Runway information	Aerodynamic coefficients
Observer locations	Procedural steps (approach and departure)
Arrival routes	Fixed point profiles
Departure routes	Grouping details
Calculation input	Default weights
Aircraft type & weight (departure)	Engine coefficients
Airport, runway, route to use	NPD data
Parameter to be calculated (L_{eq},L_{den} $L_{A_{max}}$, SEL)	Spectral classes
Grid size	**Population data**
Atmosphere parameters (Temperature and humidity)	**Topographical data**
Lateral dispersion	

From 3.2 it can be seen that there are three calculations steps. The two major steps are the flight path construction & segmentation and the event noise calculations. The construction of the flight path is very

important in order to determine the power setting P and the distance to the observer d. Moreover the NPD tables are adjusted when the atmospheric conditions are different than the reference conditions. The next subsections will describes these steps in the calculation is more detail.

3.1.1. Flight path construction and segmentation

The flight path is determined in NIROS using the input given by the user and the ANP database. The ground track (horizontal flight path) has to be defined by the user. When radar data is available this can be used, otherwise the approach and departure charts defined in the Aeronautical Information Publication (AIP) of the International Civil Aviation Organization (ICAO) are used. An example can be found in appendix C. If new ground tracks are considered, these can be created. The ANP database includes procedural steps for approach and departure, this is used to create the vertical flight profile. For each aircraft and weight class a separate flight profile is given in the database.

In NIROS segmentation of the flight path is used; the path is divided in straight line segments which represent the flight path to simplify the calculations. At the end of each segment four flight parameters are calculated i.e. height z, velocity V, bank angle ε, power setting P. The power setting is often equal to the corrected net thrust F_n/δ. Here F_n is the net thrust per engine in lbf and δ is the ratio between the ambient air pressure and the standard air pressure at sea level. The aircraft height z will be used to determine the distance to the observer. This height will be adjusted when elevation data is known according to:

$$z' = z - z_0 \tag{3.1}$$

When the entire segmentation is executed, this will create the three dimensional flight path. This path consists of a list of (x, y, z) points with their corresponding flight parameters. The flight path segments together with the segment values for power setting, will at the end be used to determine the perceived noise for observers located on the ground.

This segmentation is thus executed using the procedural steps defined by the ANP data and the user information regarding the ground track. Figure 3.3 gives an impression of the segmentation in NIROS using the ground track and flight profile.

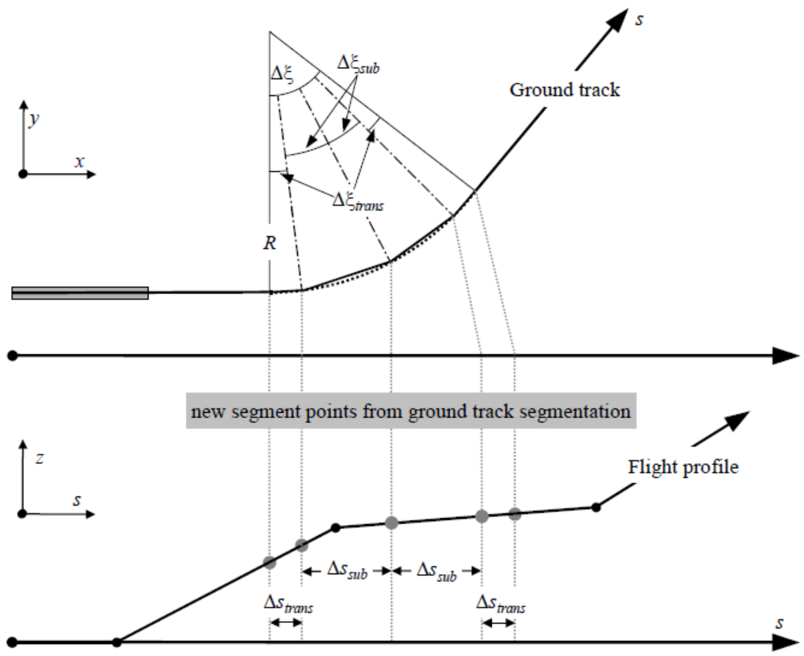

Figure 3.3: Flight segments in NIROS [15]

Firstly, segments are inserted using requirements of the ground track. After this the flight profile is segmented. Combining these two will give the segmentation of the flight path.

The construction of the flight profile will have a big influence on the predicted aircraft noise. In these calculations the corrected net thrust (power setting) will be calculated when this is not given in the ANP database for the procedural step. The data used for the determination of the corrected net thrust are the aerodynamic coefficients and engine coefficients.

The flight profile is constructed using six procedural step types (takeoff, climb, accelerate, descend, land or decelerate). For each of these procedural steps, separate segmentation approaches and formulas are given. For instance for the takeoff step type, the takeoff ground roll distance s_{TOG} is calculated using the corrected net thrust, weight data and flap deflection information and is corrected for headwind and runway gradients. Dependent on the information available per procedural step (velocity, altitude, engine parameters etc.) some flight parameters need to be calculated. This at the end will create the entire vertical flight profile. For each segment the end segment parameters are equal to the begin parameters of the next segment.

For straight ground track the flight profile construction can be done independently of the ground track. However turns in the ground track might affect the climb, necessitating incorporation of the effect of turns when defining the flight profile. The bank angle is defined as:

$$\varepsilon = \tan^{-1} \frac{2.85 \cdot V^2}{r \cdot g} \tag{3.2}$$

Where r is the turn radius and g the acceleration due to gravity. The bank angle will be used in the calculations of the flight path and corrected net thrust.

The ANP includes also fixed point profiles (so different than the use of procedural steps) however these are only used when there is a lack of data for the procedural steps. This option is not preferred and will decrease the accuracy of the method.

In conclusion the construction of the vertical flight path will have a big influence on the power setting and the flight path and consequently on the predicted noise using the NPD tables.

3.1.2. Event noise level calculation

For the calculation of the segment noise level from the NPD tables the power setting P, in this case equal to the corrected net thrust F_n/δ, and the observer distance d calculated during the flight path construction and segmentation calculations are needed. As discussed in the previous section the power setting will be calculated at the begin and end of each segment. P of a segment is determined as:

$$P = \sqrt{P_1^2 + \frac{q}{\lambda} \cdot (P_2^2 - P_1^2)} \tag{3.3}$$

In this equation P_1 is the power setting at the end of the segment and P_2 is the power setting at the begin point of the segment. q is the distance between the end point of the segment and the point closest to the observer perpendicular to the segment. λ is the length of the flight path segment.

Observer locations can be defined manually or a grid is applied. Each grid point equals an observer. The observer distance d to a segment will be determined using geometry and is generally equal to the minimum slant range (perpendicular to the flight path). However if the observer is behind or ahead the ground track, d is the minimum distance to the segment.

When the NPD table values do not match exactly with the power setting and/or the observer distance, the noise metric values are interpolated. Furthermore the NPD tables from the ANP database are adjusted for the atmospheric conditions (temperature T and relative humidity RH) if deviating from the reference atmospheric conditions.

The segment event levels are calculated using equation 3.4 for the A-weighted $L_{max,seg}$ and equation 3.5 for the SEL value per segment.

$$L_{max,seg} = L_{max}(P,d) + \Delta i(\varphi) - \Lambda(\beta,l) \tag{3.4}$$

$$L_{E,seg} = L_{E\infty}(P,d) + \Delta_V + \Delta i(\varphi) - \Lambda(\beta,l) + \Delta_F \tag{3.5}$$

Where $L_{E\infty}(P,d)$ and $L_{max}(P,d)$ are determined using the NPD database. The correction factors are:

- $\Delta i(\varphi)$ for engine installation effects
- $\Lambda(\beta,l)$ for lateral attenuation
- Δ_V the duration correction
- Δ_F for the finite segment

These correction factors are applied to include propagation effects such as ground attenuation. The duration correction is done to account for the difference in aircraft velocity between the measurements and the aircraft used. The NPD data are given for an aircraft velocity of 160 knots. Moreover the engine installation effects resulting in lateral directivity of the noise are included. The lateral attenuation correction factor accounts for the sound propagating to the side of the flight track. All NPD tables as used by NIROS are based on steady straight flight on an infinite flight path. Thus a correction has to be applied to account for the finite segments and to enable curves in the flight path.

The total event noise $L_{A_{max}}$ and SEL for an observer are calculated according to the equations 3.6 and 3.7 respectively.

$$L_{A_{max}} = max(L_{max,seg}) \tag{3.6}$$

$$SEL = 10 \cdot log(\sum_{seg} 10^{L_{E,seg}/10}) \tag{3.7}$$

In the SEL equation the summation is taken over all the segments contributing significantly to the noise level. Thus having significant $L_{E,seg}$ level for the observer. NIROS generates noise contours using all event noise values and the defined grid. In these noise contours all navigational aids and the route of the aircraft are also shown.

3.2. PANAM

The Parametric Aircraft Noise Analysis Module (PANAM) is a prediction model developed by DLR. This model was developed for the prediction of overall aircraft noise to enable comparative design studies. It is also used to identify promising low-noise technologies at early design stages.[6] PANAM is based on the principle of the simulation of all individual noise sources. The model is semi-empirical, it predicts the noise using individual source models. These source models are based on both empirical and analytical expressions. The noise sources in PANAM are modelled parametrically. The model requires several inputs to model each noise source. The fact that each noise source is modelled separately makes it possible to investigate the individual influences of the operational conditions and settings on the components produced noise. [4]

PANAM is mainly used to predict the noise of new aircraft configurations or flight procedures. This is why the program simulates the noise produced by one aircraft noise event (approach or departure). The model predicts the noise sources of an aircraft separately before combining them. Figure 3.4 shows the calculation steps within PANAM.

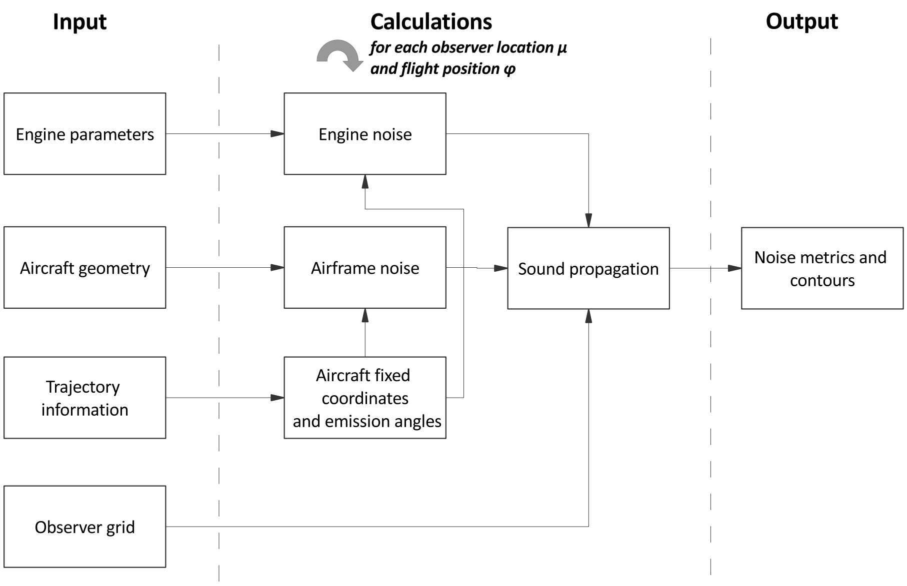

Figure 3.4: Simplified PANAM model flowchart

In order to complete these calculations many different parameters are needed. These parameters include the aircraft geometry, observer information, engine parameters, engine stage information and flight trajectory information. All these inputs are described in Appendix A.

PANAM thus requires many inputs for the calculations. Manufacturers do often not share this detailed information because of confidentiality. When this is the case, data can be obtained from experiments or it can be estimated. The program PrADO [12] and the DLR model for the generation of gas turbine configurations (similar to GasTurb [37]) can be used when not all information of an aircraft is known. PrADO can be used to determine the aircraft geometry or flight dynamics. However when input data is estimated the accuracy of the noise prediction models will decrease.[26]

The airframe noise module predicts the noise produced by the wing, slats, flaps, landing gear and spoilers. In the engine noise simulation the jet, fan and liner noise are calculated.

The outputs of PANAM are the overall noise levels. Various noise metrics can be calculated using PANAM. These include $L_{A_{max}}$, EPNL, SEL and L_{eq}. Moreover time-level-histories for observers can be generated. The standard output also includes the noise produced by the different noise sources. The next sections will discuss the calculation steps of PANAM in more detail.

3.2.1. Flight path construction

PANAM is made to evaluate three-dimensional flight trajectories. The observer and aircraft are defined in a vector notation within the earth-fixed coordinate system (see figure 3.5). The flight path is discretised into quasi-stationary positions $\varphi(x, y, z)$. Within this time increment the configuration, location, orientation and operating conditions are assumed to be constant.[4]

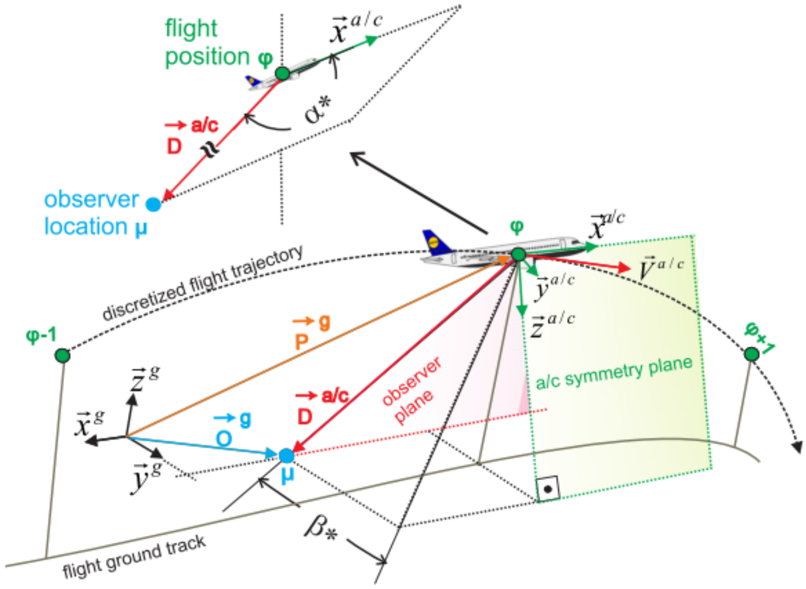

Figure 3.5: PANAM coordinate systems [4]

3.2.2. Engine noise in PANAM

In PANAM the jet noise is modelled using the model of Stone [52] and fan noise is predicted with the model of Heidmann [30]. The latter model is modified in the same manner as was done in studies executed by NASA. This in order to adjust the model to be applicable for a wider range of fan pressure ratios, tip speeds and bypass ratios. Due to these adjustments, PANAM can be used for modern turbofans with bypass ratios of up to 15.[7] The model is able to predict the fan noise spectrum within 4 dB uncertainty, which holds for low and moderate tip speed fans.[23] To account for acoustic liners, the method of Moreau, Guérin and Busse is used.[7]

Jet and fan noise are predicted in a sphere of 1m for the emission angles α^* and β^*, see figure 3.5. The station numbering used in PANAM is according to figure 3.6. At these places parameters such as velocity, temperature, area and mass flow have to be known in order to compute the noise (see appendix A).

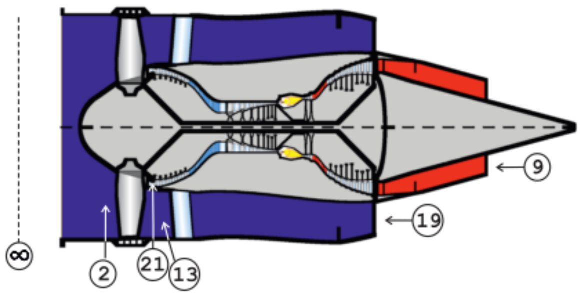

Figure 3.6: Station numbering for turbofan and turbojet noise calculation [5]

3.2.3. Airframe noise in PANAM

Where other semi-empirical models often use the method of Fink for airframe noise modelling, PANAM applies a self-established method. The noise source models are based on recent data from wind tunnel and flyover measurements. The wing is divided in segments. This enables modelling the noise produced by unconventional airframes. Furthermore landing gear, trailing edge and leading edge high-lift devices and spoilers are included using DLR models.[6] All equations for both engine and airframe noise can be found in [5].

3.2.4. Sound propagation

The Sound Pressure Level (SPL) for a range of frequencies is predicted on a reference sphere around the aircraft.[5] Sound propagation effects have to be accounted for to calculate the noise received by the observer. These effects include geometrical spreading, atmospheric absorption, convection effects like convective amplification and frequency Doppler shift and ground attenuation.[4]

Atmospheric absorption is accounted for according to the American National Standards Institute (ANSI) standard [44]. The ground reflection methodology can be specified in PANAM. The default setting is the AzB ground reflection calculation. Other options are Nilsen, Flula(1993), SAE(1981) and Delany. Free field conditions can also be simulated by not choosing one of these settings. The default ground reflection setting is the ground reflection method applied by the former empirical noise prediction model AzB [17] (more information in Appendix B).

The received SPL of an observer can be integrated over time to calculate the SEL or EPNL. In addition, when using a grid of observers, the model can be used for the calculation of noise contours.

3.3. Discussion methodology differences

As described in the previous sections, NIROS and PANAM use different methods for the prediction of aircraft noise. They are intended for different purposes: NIROS for assessing the noise produced by multiple flyovers and PANAM for a single event.

The main difference between the two models is the application of NPD tables versus the source modelling of all separate noise sources. This will have a large influence on the predictions. In PANAM, configuration changes will have an influence on the noise prediction. This will not be the case when using NPD tables. The use of NPD tables will result in accurate predictions of flyovers similar to the certification situation. However it might result in large errors when the operational situation is changed.

In NIROS each aircraft has its own flight profile defined within the ANP database for both the approach and departure. The user can choose the ground track. This flight path will be constructed and segmented in order to calculate the power setting. This power setting and the distance to the observer will be used to determine the noise using data from NPD tables. The flight path construction is very different in PANAM. In this model the flight path is an input given by the user. When no flight data is available other models such as PrADO could be used to simulate a flight path. PANAM itself discretizes the flight path in order to simulate the noise produced by the aircraft. The main difference between the flight paths used in both models is the fact that for PANAM arbitrary flight profiles are possible.

Another difference lies in the calculation of propagation losses. In NIROS all propagation losses are accounted for in an implicit manner. This means that the NPD tables already include atmospheric absorption for standard atmospheric conditions. However several correction factors are applied to account for effects such as lateral attenuation (ground reflection), installation effects etc. These formulas are all empirical and are thus an approximation of the real sound propagation effects. PANAM incorporates all sound propagation effects separately. This means that Doppler shift, geometrical spreading and atmospheric absorption is calculated after all noise source calculations are executed. In PANAM the ground reflection model can be chosen by the user. However the default choice is the AzB implementation. PANAM and NIROS thus have both their own way of implementing sound propagation effects. This might result in differences between the noise predictions on the ground of both models.

The described three major differences i.e. source modelling, flight path construction and noise propagation, will be examined closely when analysing the noise predictions of both models in the next chapters.

4

Simulations in NIROS and PANAM

This chapter describes the simulation and presents the resulting predictions of NIROS and PANAM. In this simulation both PANAM and NIROS are used to estimate the noise produced by an A319 at Schwerin-Parchim airport (EDOP). The results of both models will be examined to establish the differences between the two models. The first section 4.1 discusses the simulation requirements. In section 4.2 the set-up of the simulation case is described in more detail. Then the results of both the approach and departure simulations are given in section 4.3. Finally in section 4.4 intermediate conclusions are drawn. These conclusions will be the focus of the remaining research.

4.1. Simulation requirements

In order to assess the differences, each simulation in both models should have comparable input without undermining the models methodology. As can be seen in table 4.1 NIROS has less input variables which can be varied by the user than PANAM. This is because of the fact that the data NIROS uses for its calculations originates mostly from the ANP database.

Table 4.1: Input parameters PANAM and NIROS

PANAM	**NIROS**
Airframe geometry and settings	Aircraft type
Atmospheric conditions	Atmospheric conditions
Engine (thrust profile, type of engine etc.)	
Flight path	Ground track and weight
Type of ground reflection method	Ground elevation

NIROS uses the ANP database, which will lead to differences in the input for the simulations. The aerodynamic and engine coefficients in this database can be changed. However doing this will undermine the applied method by NIROS. All these coefficient and constants are empirically obtained. For this simulation it was chosen to not vary anything inside of the ANP database. Changing these coefficients will change the method on which NIROS is based.

Moreover, the simulation cases have to be within the capabilities of the methods and should reflect the purpose and use of the models. Both models have their limitations. The use and purpose will be taken into account in the simulations in order to establish a fair comparison of the models. This is also why it is chosen to use only single flyover events. Although NIROS is capable of predicting the noise of multiple flyovers only single flyover events are compared because of the scope of PANAM.

Finally realistic cases should be modelled. The simulation should be based on a flight situation representing the reality. This means that the aircraft should be an often used one and the flight profile should be a common used procedure which makes it possible to compare the predictions with flyover data.

4.2. Simulation set-up

This section will describe the situation considered in the simulations. NIROS and PANAM will be applied in both an approach and a departure situation. The main simulation parameters can be found in table 4.2. In section 4.2.1 the implications of the chosen aircraft are discussed. The flight path is described in section 4.2.2. Both models have their own way of calculating the atmospheric propagation, these conditions are described in section 4.2.3. Section 4.2.4 describes the noise metrics used and how the noise contours will be made.

Table 4.2: Simulation parameters

	Simulation set-up
Aircraft	A319
Airport	Schwerin-Parchim (EDOP)
Ground track	Straight (no variation in y-direction)
Temperature	15 ° C
Relative humidity	70 %
Noise metric simulated	SEL and $L_{A_{max}}$

4.2.1. Simulated Aircraft

The aircraft chosen for all the simulations is similar to the Airbus A319. A picture of this aircraft can be found in figure 4.1. This is a commercial aircraft with a seating capacity up to 156. The maximum range the A319 can fly is 6950 km and therefore the A319 is used for short to medium range flights. [1]

Figure 4.1: A319 [1]

The choice for this aircraft is based on two reasons: the A319 is widely used and for PANAM all input data is known. As described earlier, PANAM needs very detailed inputs. Furthermore measurement data is available which can be used to validate the simulation results. The version used in PANAM is the A319-100. This aircraft has CFM56-5A5 engines. Unfortunately in NIROS this A319 version is not part of the database. This is often the case when simulating aircraft in NIROS because the database incorporates around 140 specific types of aircraft. The normal procedure is then to choose an aircraft most similar to the type of aircraft wanted in the simulation. NIROS can simulate another A319, the A319-131 with V2522-A5 engines. In table 4.3 the differences between the two types of engines are given. The rated output and overall pressure ratio is of comparable magnitude. However the bypass ratio of the engine of the NIROS aircraft is lower. This might cause some discrepancies in the predicted noise. This issue will be discussed in section 5.2. The airframes of both aircraft are the same and the engines are thus comparable.

Table 4.3: Engine specifications [20]

Characteristic	A319-100 CFM56-5A5	A319-131 V2522-A5
Rated output (kN)	104.53	102.66
Bypass ratio	6	4.88
Overall pressure ratio	25.1	25.6

The aircraft simulated in PANAM has an aircraft weight of 45000 kg. In NIROS it is only possible to choose the weight during the departure. For NIROS also a low weight option is chosen. In NIROS this aircraft has a weight of 125900 lb which is around 57107 kg.

4.2.2. Flight path

In PANAM it is possible to predict the noise of every arbitrary 3D flight path. It was chosen to use a standard procedure which is often used for the A319 in Germany. This means that for the approach the Low Drag Low Power (LDLP) and for the departure a modified IATA procedure with flexible thrust setting (MODATA-FLX) will be modelled. These flight paths are known due to the flight recorder data of measurements at Parchim airport in 2006 [43].

When using NIROS the flight profile will be automatically chosen. For each possible aircraft and weight class the database has one standard profile. The ground track can be specified by the user according to the Aeronautical Information Publication (AIP). However in this simulation a straight ground track will be used in NIROS in order to be able to compare the results with PANAM. To verify this assumption a check is done on differences with the (curved) ground tracks for approach and departure used in NIROS and modelled according to the AIP. These are realistic ground tracks and are used by normal aircraft. For Parchim airport these are the BKD2E and BKD5H at runway 06. The ground tracks and the results are given in Appendix C. The ground track at Parchim airport had a negligible effect on the noise prediction results of NIROS and thus a straight ground track can be used for this research.

In figure 4.2 the vertical profiles of the approach as used for the simulations are given. There is quite some difference between the flight profiles, mainly in the first phase of the approach. The reason for this is that the ANP database has limited approach profiles due to a lack of NPD data of approaches. For most aircraft in this database a long straight segment followed by a 3 ° decline is used. In the coming years these profiles will be adjusted.[15]

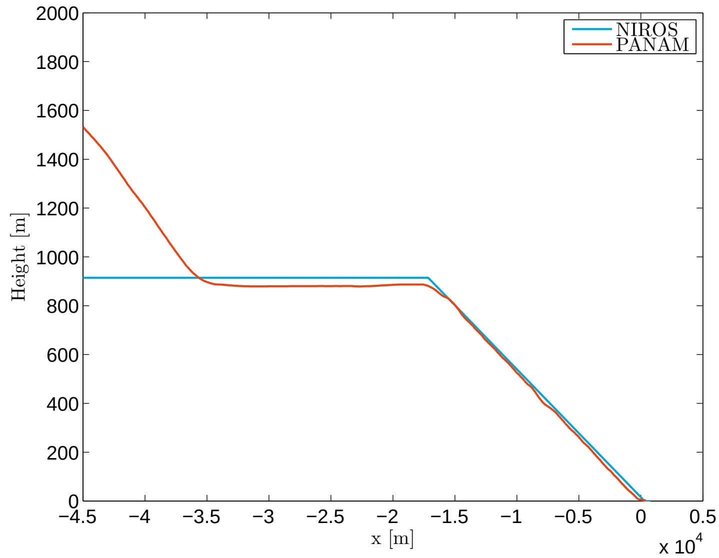

Figure 4.2: Height of flight profiles approach

In figure 4.3 the vertical profiles of the departure are shown. These profiles slightly differ. The MODATA profile of PANAM is higher just after take-off. However this profile has a lower altitude at the end of the flight manoeuvre.

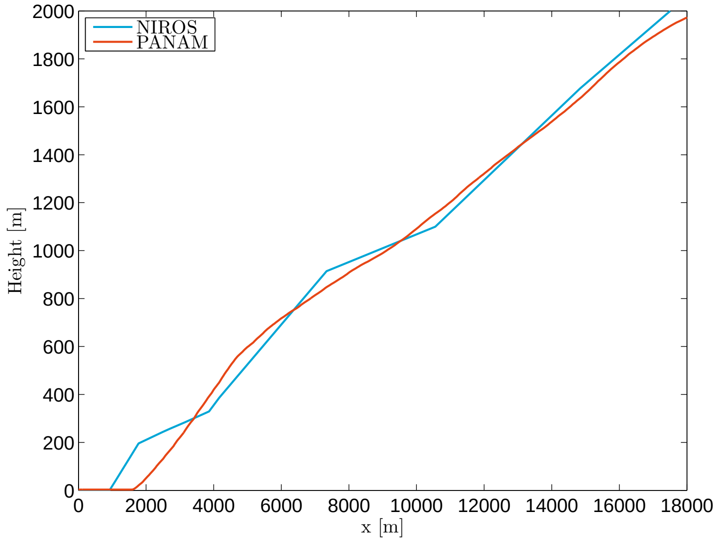

Figure 4.3: Height of flight profiles departure

To execute PANAM also information regarding the configuration is needed. Figure 4.4 shows the flap, slat, spoiler and landing gear extension during the approach. For landing gear and spoilers the location of deployment is given. The flaps and slats have several positions as shown in degrees.

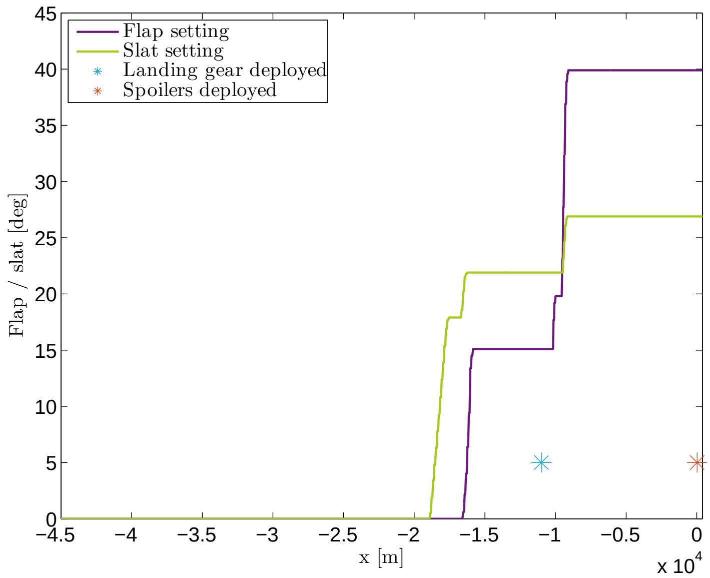

Figure 4.4: Flap, slat, gear and spoiler deployment PANAM LDLP

During the departure the gear is retracted at 1940 m. However exact data for flap and slat angles was not available for PANAM. In consequence the flaps and slats are excluded during the modelling of the departure. The absence of flaps and slats modelling has been checked in a simulation with fictitious flap and slat angles. The presence and retraction of high lift devices had no influence on the predicted noise levels during the departure. Therefore it was concluded that it is not necessary to include the flaps and slats settings during the departure in this case.

4.2.3. Atmospheric conditions and ground reflection

The atmospheric conditions used in the simulations are equal to the standard atmospheric constants. This means that the temperature T in the simulations is 15 $°C$ and the relative humidity RH is 70 %.

The default setting of PANAM is to calculate ground reflection with the AzB 2006 model and is used in the simulations. NIROS applies a correction factor to take into account lateral attenuation. This correction factor is based on the AIR-5662 standards made by the Society of Automotive Engineers (SAE).

4.2.4. The noise metrics considered for the model comparison

As mentioned in section 4.1 only single event noise metrics are used. The standard noise metric is the Sound Pressure Level (SPL) described in equation 4.1.

$$SPL = 10 \log \frac{p_e^2}{p_{e_0}^2} \tag{4.1}$$

In this equation, p_e is the effective sound pressure and p_{e_0} is the reference effective sound pressure ($2 \cdot 10^{-5}$ N/m^2). To approximate the response of the human ear (hearing range see figure 4.5), A-weighting is applied. Figure 4.6 shows the A-weighting curve. The correction $\Delta L_A(i)$ must be added to the SPL level, for each 1/3 octave frequency i, as:

$$L_A(i) = SPL(i) + \Delta L_A(i) \tag{4.2}$$

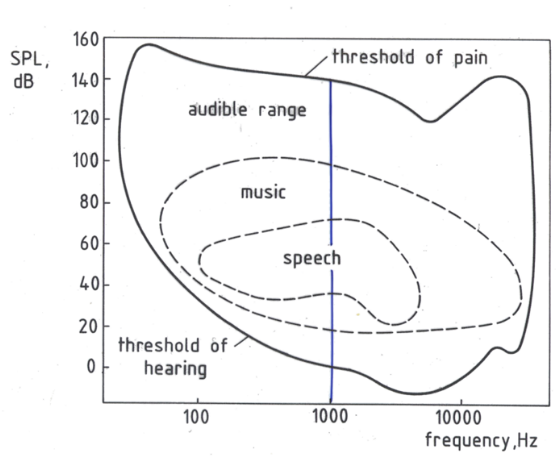

Figure 4.5: Hearing range of a human [49]

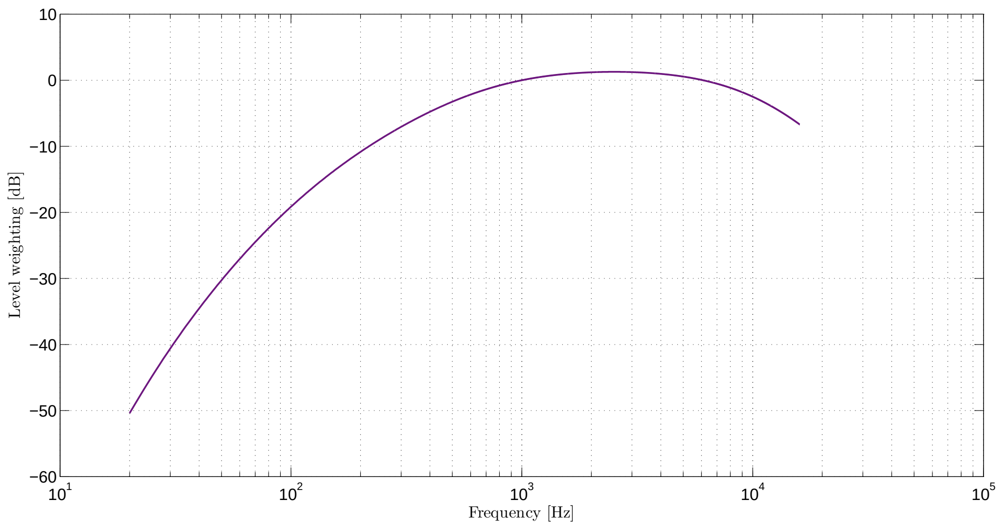

Figure 4.6: A-weighting

The overall A-weighted sound level (in dBA) is defined as:

$$L_A = 10\log\sum_i 10^{L_A(i)/10} \tag{4.3}$$

In this research $L_{A_{max}}$, the maximum value of L_A, is used as an output metric. The second metric used, the A-weighted Sound Exposure Level (SEL) in dBA, is given in equation 4.4.

$$SEL = 10\log\left[\frac{1}{T_1}\int_0^T 10^{\frac{L_A(t)}{10}}\,dt\right] \tag{4.4}$$

This is the time integrated version of the L_A metric. Both the SEL and the $L_{A_{max}}$ will be used as noise metrics to compare NIROS and PANAM.

A grid of observers is used to compute the noise contours. For NIROS the standard setting of the grid is 40km by 40km. A grid spacing of 100m between each grid point is used. The same grid spacing is used in PANAM. The width and height of the grid is adjusted in PANAM in order to lower the computation time.

With this observer grid, the noise will be assessed in both the lateral and longitudinal direction. These directions are showed in figure 4.7. The longitudinal direction is the noise in the direction of the flight path. Lateral noise is defined perpendicular to the flight path.

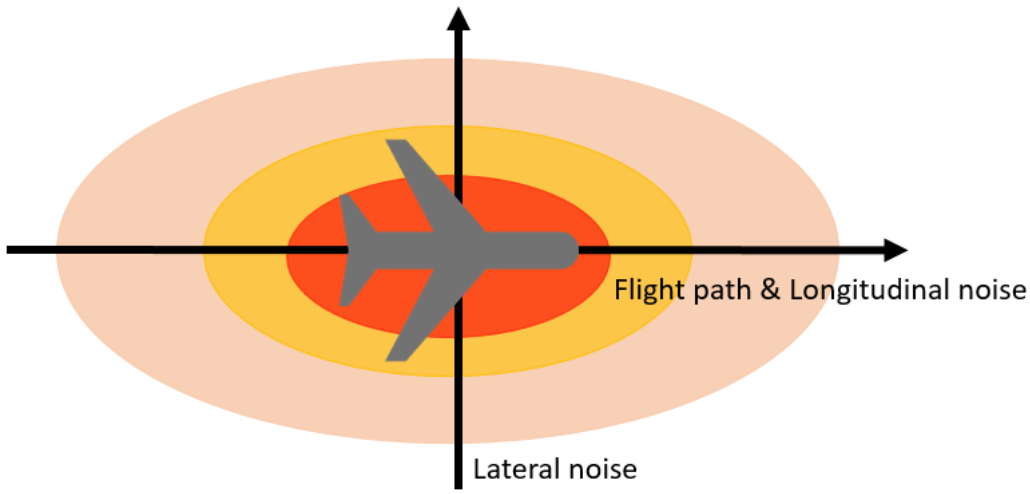

Figure 4.7: Longitudinal and lateral noise

4.3. Simulation results

Using the simulation set-up as described in the previous section the simulations were performed. This section will give the results of the simulations. In section 4.3.1 the results of the predictions of the approach in NIROS and PANAM are given. Section 4.3.2 shows the noise prediction results of the departure.

4.3.1. Approach

For the approach a straight ground track is used. In NIROS the vertical profile is generated automatically. The procedural steps are used for the segmentation as described in 3.1.1. NIROS calculates the velocity and corrected net thrust (power setting). Figure 4.8a shows the total thrust and calibrated airspeed (CAS) calculated within NIROS for the approach. The corrected net thrust is converted from lbf to kN and multiplied by 2 to account for both engines. The peak at the end is the reverse thrust during the landing. The thrust and true airspeed (TAS) corresponding to the LDLP approach procedure in PANAM are given in 4.8b. For the simulations the assumption is made that the TAS is equal to the CAS. This is only the case when the atmospheric conditions are equal to the standard sea-level reference conditions according to equation 4.5 .[50]

$$TAS = \sqrt{\frac{2\gamma}{\gamma-1}\frac{p}{\rho}\left[\left[1+\frac{p_0}{p}\left[\left(1+\frac{\gamma-1}{2\gamma}\frac{\rho_0}{p_0}CAS^2\right)^{\frac{\gamma}{\gamma-1}}-1\right]\right]^{\frac{\gamma-1}{\gamma}}-1\right]} \tag{4.5}$$

In this equation γ is the ratio of specific heats, ρ the density and ρ_0 the sea-level density and p and p_0 the pressure and sea-level pressure. When assuming the sea-level conditions p=p_0 and ρ=ρ_0 and thus the TAS is equal to the CAS.

As can be seen the thrust and TAS lines are not smooth. This is because the data used within PANAM result from flight recorder data(from the Parchim measurement campaign [43]) and from engine data (from measurements of DLR). The flight recorder data is used to define the exact trajectory and the flap, slat and landing gear settings. Moreover the engine data is used to determine most engine parameters such as the engine stage information and engine design parameters.

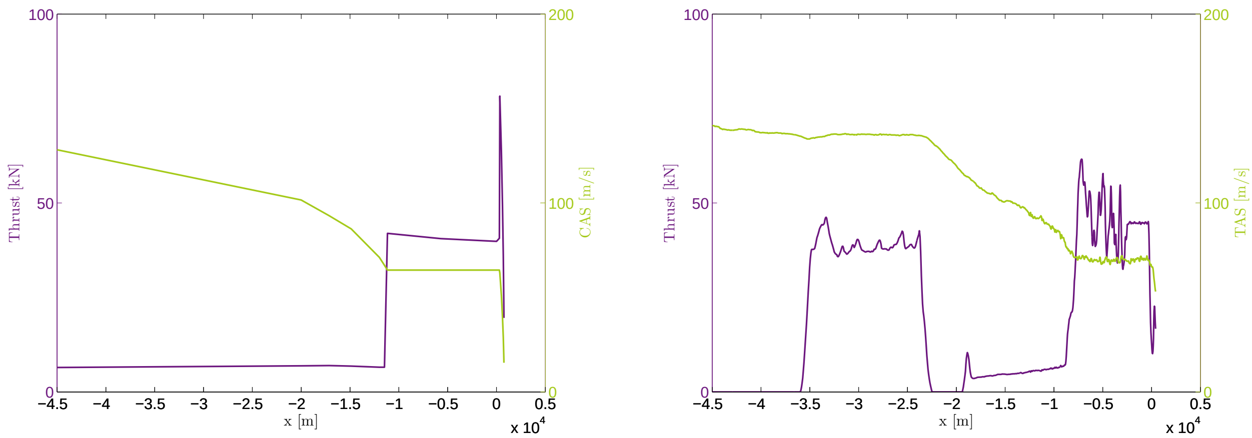

(a) NIROS STANDARD (b) PANAM LDLP

Figure 4.8: Velocity and thrust profiles

Both models use a different velocity and thrust profile for the approach. The thrust of PANAM's LDLP profile has two major peaks and is more unstable than the thrust calculated by NIROS. The velocity of the simulated aircraft of PANAM is higher at the start of the approach. These differences will be discussed more extensively in chapter 5.

Figure 4.9 shows the noise contours in SEL and $L_{A_{max}}$. When comparing the noise contours of NIROS with PANAM a difference in the noise level and in the lateral attenuation of the sound can be seen. This is visible for the SEL and $L_{A_{max}}$ contours. The increase in thrust of PANAM has a huge influence on the noise contour laterally. Moreover the extension of high lift devices and landing gear can slightly be distinguished. This will be further investigated in section 5.3. This is clearly not the case in the simulations of NIROS and thus the noise contours differ.

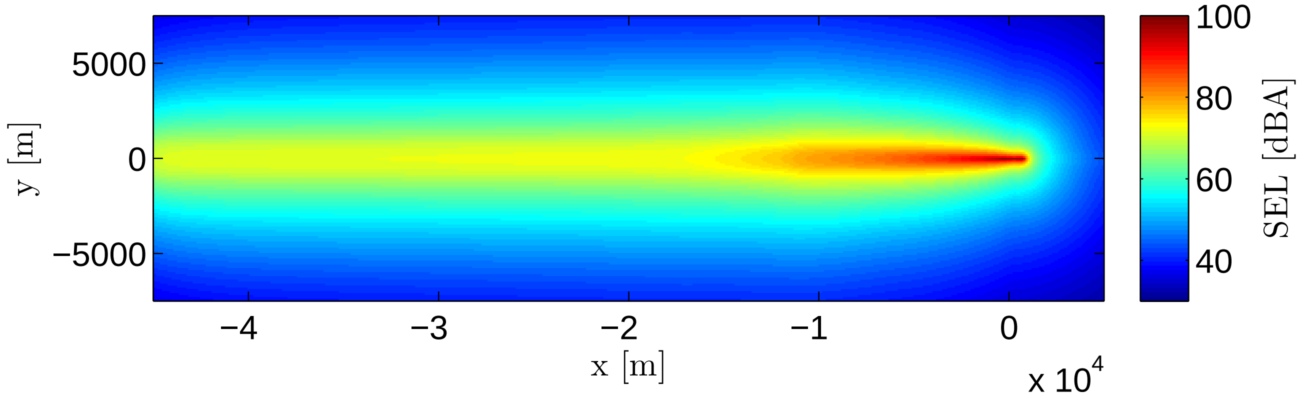

(a) NIROS SEL

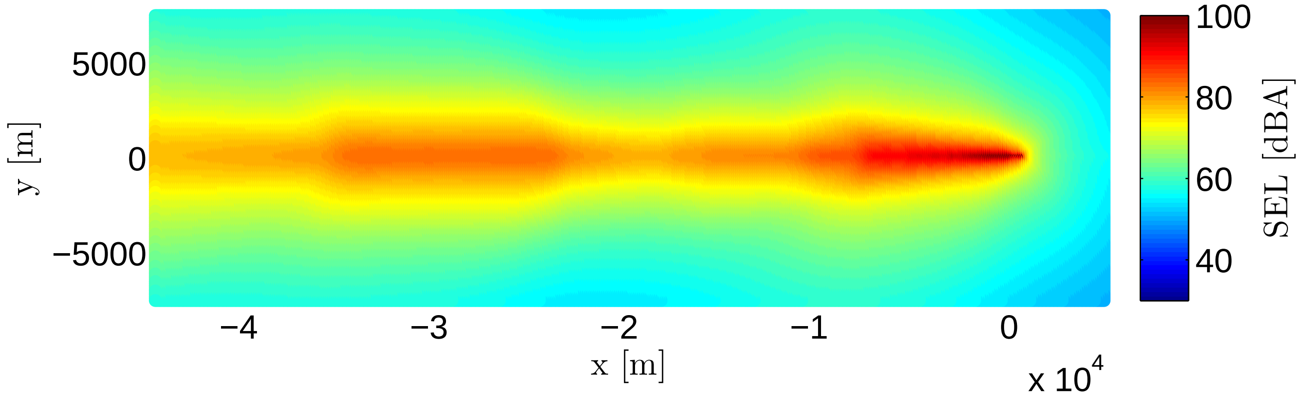

(b) PANAM SEL

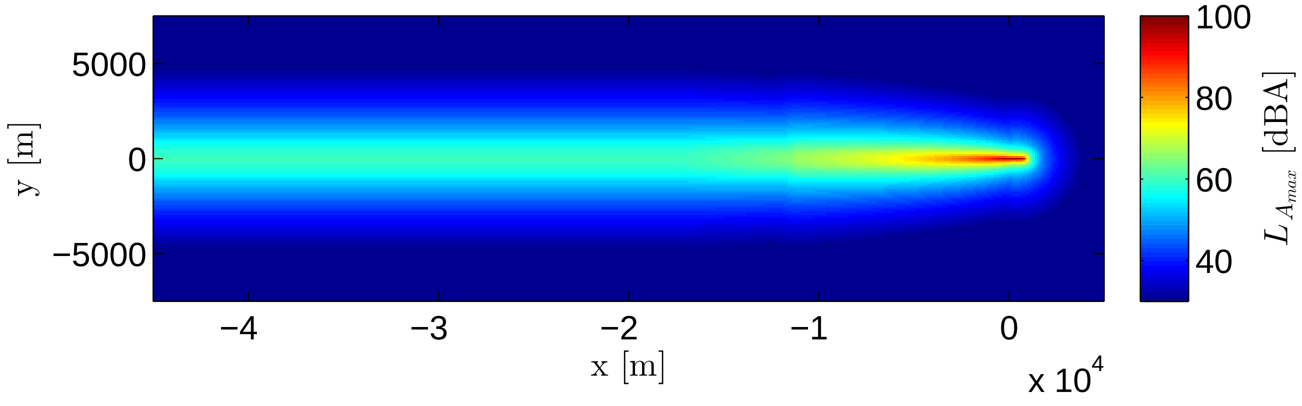

(c) NIROS $L_{A_{max}}$

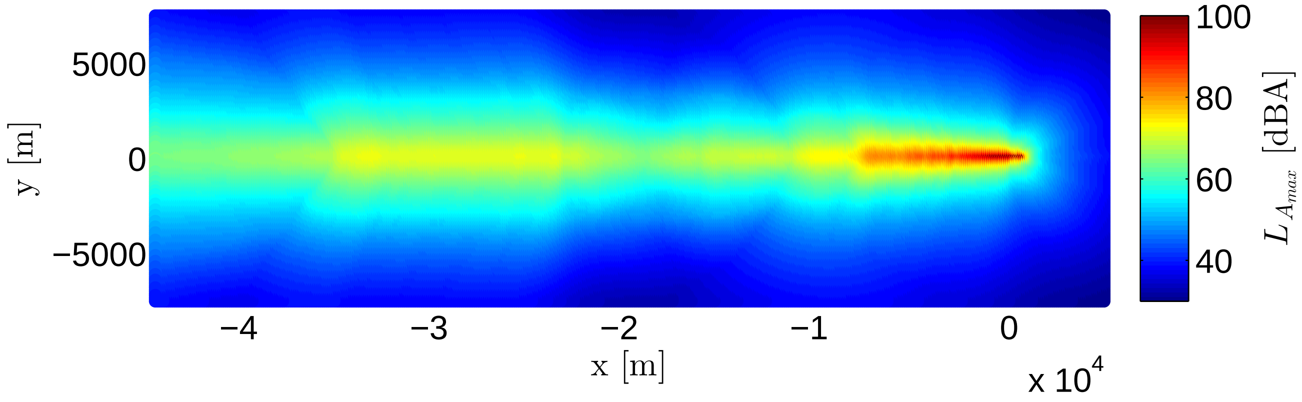

(d) PANAM $L_{A_{max}}$

Figure 4.9: Noise contours A319 approach

In figure 4.10 the SEL and $L_{A_{max}}$ levels are plotted for observers directly under the flight path. This is also done for observers on a line y perpendicular to the ground track at x is 3000 m to assess the lateral noise levels. The levels of both the SEL and $L_{A_{max}}$ of PANAM are higher for the longitudinal noise. The SEL levels directly under the flight path have around 7.7 dBA offset. The $L_{A_{max}}$ difference is on average 8 dBA. However around the same location both models predict the maximum noise levels and the trend is similar. Another observation is that the landings are not exactly at the same location. As a result the maximum noise is also at different locations in the graph. The lateral noise predicted by PANAM is also higher. Moreover this noise level decreases slower than the lateral noise as predicted by NIROS.

Both thrust levels have an increase around 40 kN during the approach. For the PANAM simulations this is around -35000 m and for NIROS this is just before -10000 m. In the figure it can be clearly seen that this has more effect on the noise level in PANAM than in NIROS.

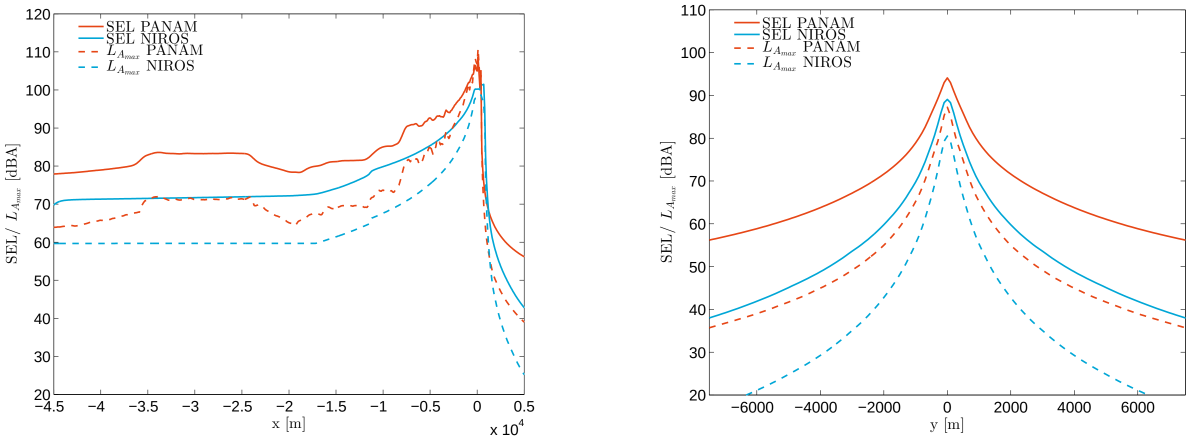

(a) Longitudinal noise directly under the flight path

(b) Lateral noise at x= -3000 m

Figure 4.10: SEL and $L_{A_{max}}$ comparison NIROS and PANAM approach

4.3.2. Departure

In figure 4.11 the thrust and velocity of both simulations are showed. The segments of NIROS are clearly visible in these graphs. Both the thrust and TAS of PANAM look more unstable because this flight path originates from measurement data. The differences between these parameters will be extensively discussed in chapter 5.

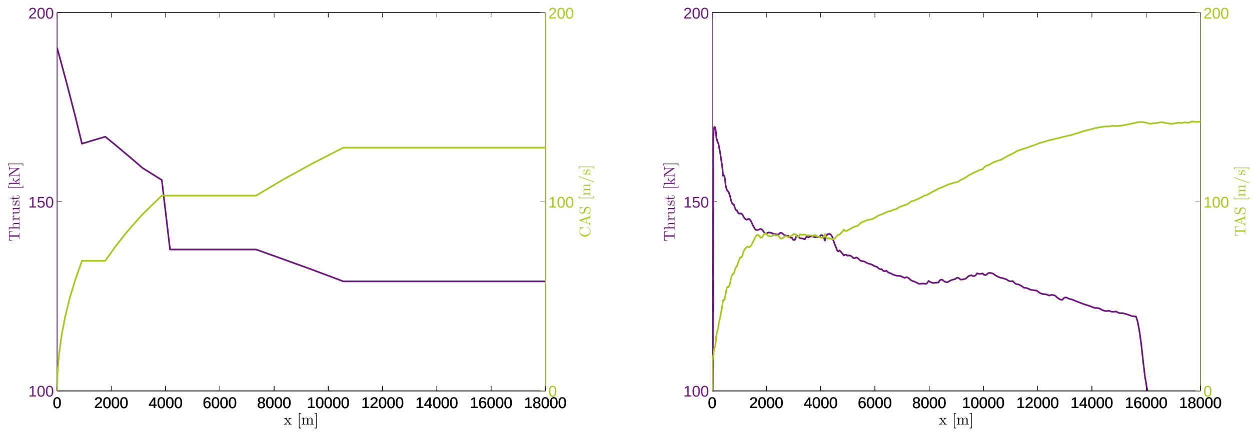

(a) NIROS STANDARD

(b) PANAM MODATA

Figure 4.11: Velocity and thrust profiles departure

Figure 4.12 shows the noise predictions calculated by NIROS and PANAM. These contours are generated for both SEL and $L_{A_{max}}$.

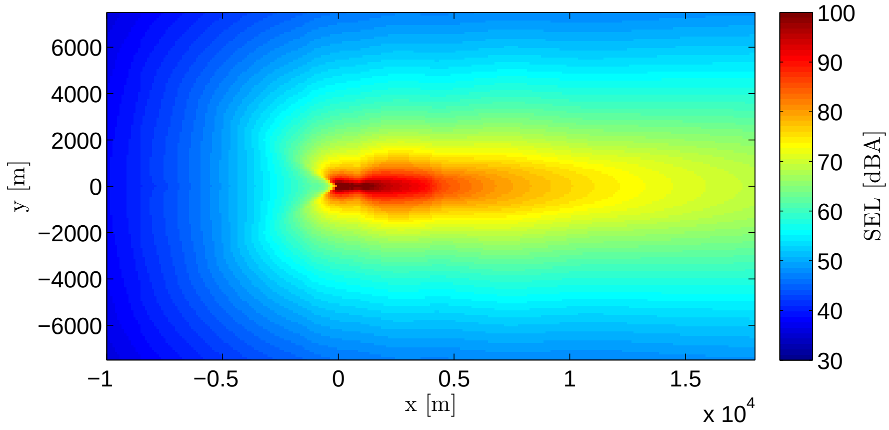

(a) NIROS SEL

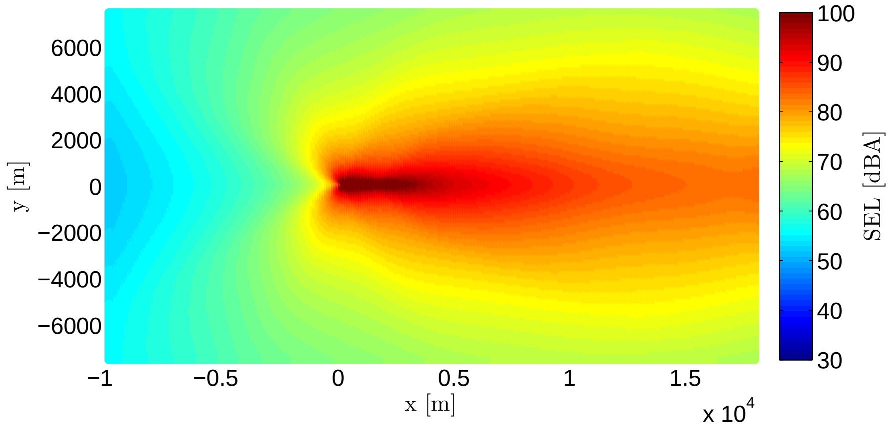

(b) PANAM SEL

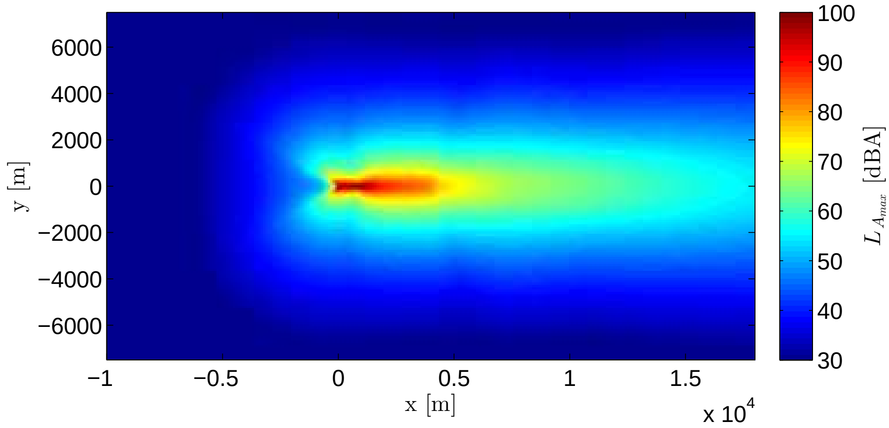

(c) NIROS $L_{A_{max}}$

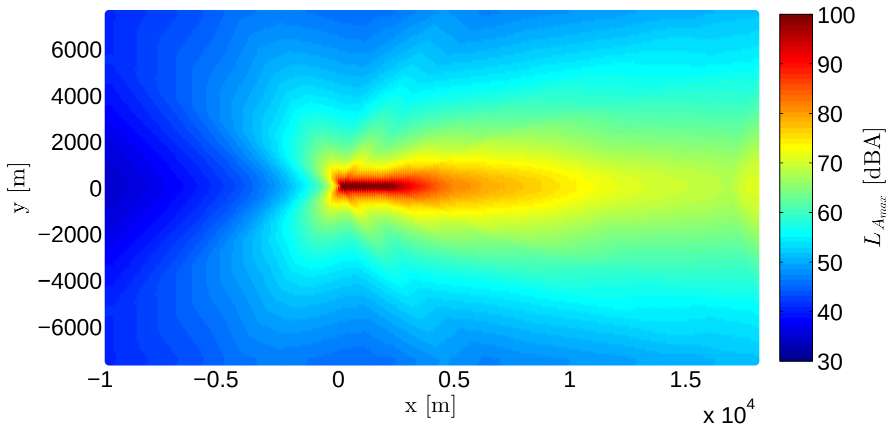

(d) PANAM $L_{A_{max}}$

Figure 4.12: Noise contours A319 departure

When comparing the PANAM SEL contour with the SEL contour of NIROS, significant differences can be seen. The observer noise levels computed by PANAM are larger everywhere. In the $L_{A_{max}}$ plots it can be clearly seen that PANAM has a larger area where the noise level is between 100-75 dBA than NIROS. Furthermore the aircraft simulated in PANAM takes off a bit later. However this can not explain the huge difference. Also the lateral noise is much higher in the predictions of PANAM.

In figure 4.13 the sound levels are given for the observers directly under the flight path. This figure also shows the lateral noise for observers at x= 3000 m. The same observations as for the approach hold; PANAM predicts higher noise levels than NIROS.

The differences between both predictions are larger than for the approach. The SEL from NIROS and PANAM differ 13.4 dBA on average for observers located under the flight path. The $L_{A_{max}}$ difference is on average 15.1 dBA for observers directly under the flight path. However the noise peaks of all the predictions are almost at the same location. The large drop in thrust of NIROS just before 5 km can clearly be distinguished in the graphs. For lateral noise PANAM also predicts higher values. The noise prediction of NIROS quickly decreases with increasing lateral distance.

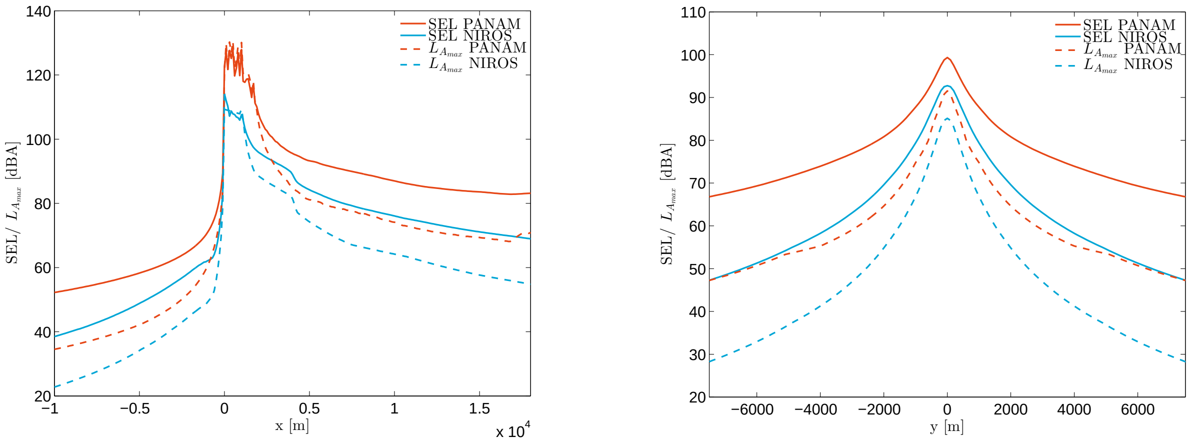

(a) Longitudinal noise directly under the flight path

(b) Lateral noise at x= 3000 m

Figure 4.13: SEL and $L_{A_{max}}$ comparison NIROS and PANAM departure

4.4. Intermediate observations

In this section the results are summarised. From the simulations four important observations can be made. These observations will be used in the remaining research. In the next chapters the results presented in this chapter will be further analysed and discussed.

Large difference in noise levels predicted During the approach and departure there is a large difference in the noise level predicted by the two models. This is the most important observation. PANAM always predicts a higher noise level than NIROS does. During the departure this difference is the largest.

Trend is similar The trend line of both predictions directly under the flight path is similar. As discussed previously there is an offset, however the predictions show almost the same locations of high noise levels.

Influence of configuration and thrust changes PANAM clearly shows variations in lateral noise during the approach due to thrust and/or configuration changes. These variations do not, to the same extent, influence the predictions of NIROS.

Small difference in landing and take-off point The take-off and landing point of the simulations are not exactly the same. The difference is small but has an influence on the predictions.

5

A detailed assessment of the differences in the predicted noise levels

In chapter 4 the results of the A319 simulations were given. In this chapter these results will be further analysed. The goal is to investigate possible explanations of the observed differences. The two model simulations are analysed in detail and the influence of input and methodology differences are discussed.

First, in section 5.1 the discrepancies in flight paths are discussed. Additional simulations are executed to identify the influence of the flight profile on the noise predictions. The influence of the different engines used in the simulations are described in section 5.2. Then the influence of the separate modelling of flaps, slats, spoilers and landing gear in PANAM are further investigated in section 5.3. Finally, the methods applied for ground reflection and atmospheric absorption in NIROS and PANAM are discussed in section 5.4 and 5.5 respectively.

5.1. Differences in flight paths NIROS and PANAM

There are some major differences in the construction of the flight path used in NIROS and PANAM. This is due to the different methods used: in PANAM it is needed to define the entire flight path upfront and in NIROS the vertical flight profile is calculated using the database. In this section the differences in the three parameters thrust, height and velocity are discussed in section 5.1.1. Furthermore the influence of these different parameters is investigated using additional simulations in section 5.1.2.

5.1.1. Thrust, height and velocity evaluation

In this section the differences between three important parameters i.e. thrust, height and velocity are discussed. These three parameters are strongly correlated to the predicted noise levels of both models.

As can be seen in figure 5.1 the thrust levels used for the simulations in PANAM and NIROS for both approach and departure differ. This difference is the highest during the approach and the end of the departure. The thrust used by the aircraft simulated in PANAM increases two times with large steps of around 40 kN. In NIROS the thrust is only increased at the end of the approach with 40 kN and during touch down with a short reversed peak thrust of 80 kN.

In figure 5.2 the differences in height between PANAM and NIROS are plotted. For the approach approximately the same height profile is used from x is equal to -35000 m onward. During the departure there are major differences in height of the aircraft. The simulated aircraft of PANAM and NIROS alternately have more height.

In figure 5.3 the differences in velocity between PANAM and NIROS are showed. Due to the larger height of the aircraft of PANAM during the approach, the velocity is also higher than the NIROS A319. During the entire approach the velocity predicted by NIROS is lower than the velocity used in PANAM. This is not the case during the departure, here the velocity in NIROS is generally higher than in PANAM.

There are thus some major differences in the parameters thrust, height and velocity. These differences are likely to cause differences in the noise predictions.

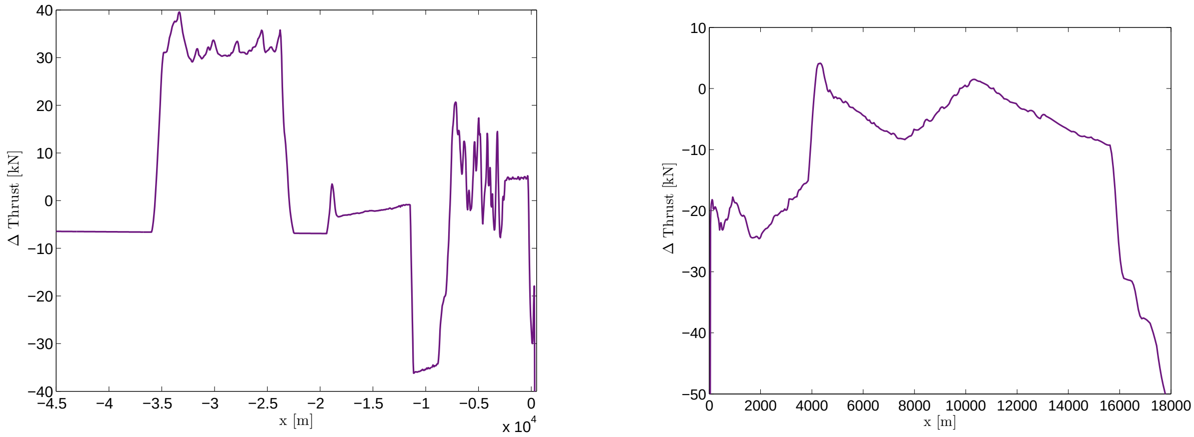

(a) Approach (b) Departure

Figure 5.1: Differences in thrust between A319 simulations in PANAM and NIROS. Positive values indicate higher thrust of PANAM and negative values indicate higher thrust of NIROS.

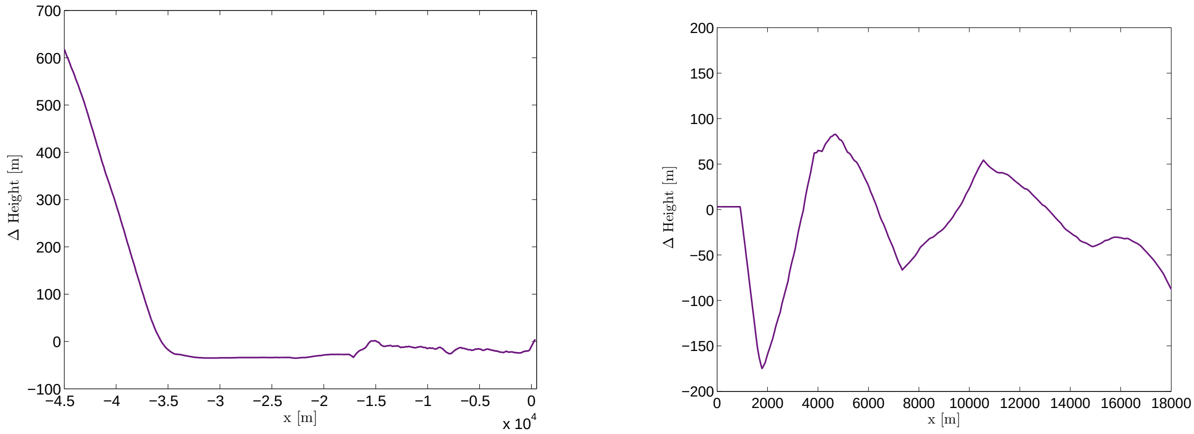

(a) Approach (b) Departure

Figure 5.2: Differences in height between A319 simulations in PANAM and NIROS. Positive values indicate higher height of PANAM and negative values indicate higher height of NIROS.

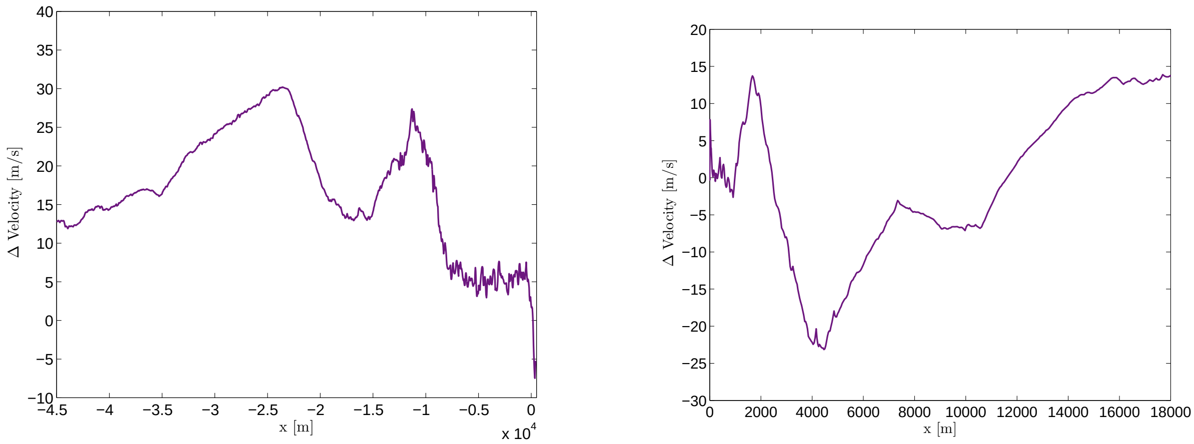

(a) Approach (b) Departure

Figure 5.3: Differences in velocity between A319 simulations in PANAM and NIROS. Positive values indicate higher velocity of PANAM and negative values indicate higher velocity of NIROS.

5.1.2. Influence of flight path differences

As discussed in section 5.1.1 there are some major differences in thrust, height and velocity used in the simulations of PANAM and NIROS. Moreover in section 4.4 it was concluded that there are differences in the take off and touch down point of both simulations. To identify the influence of the difference in vertical flight profile on the noise predictions some additional calculations and simulations are performed.

The influence of the differences in take off and touchdown point are small. The touchdown calculated for NIROS is at 300.1 m . In PANAM the aircraft lands at 252.6 m. This differences of 47.4 m will have an influence on the noise of 0.01 - 0.1 dBA. The noise levels calculated for NIROS during the approach are thus slightly shifted to the left. In the departure there is a bigger gap between the take off points of NIROS and PANAM. PANAM takes off later at 1567 m. Shifting the noise levels of NIROS with 624.8 m to the right will have an influence of approximately 1 dBA. So exactly aligning the landing and take off points shift the NIROS noise contours to the left or right.

Two approaches are used to identify the influence of the different height used in the vertical flight profiles of PANAM and NIROS. Firstly the height used in PANAM LDLP and MODATA is modelled using NIROS. The procedural steps need to be changed within the database of NIROS in order to best fit the flight path flown to the PANAM profiles. Flexibility of NIROS is hereby limited due to the procedural steps. Therefore it is not possible to exactly replicate the PANAM profiles. Only for the departure it was possible to create approximately the same procedure. This had a maximum influence of ± 5 dBA close to the runway.

The second approach is to model the vertical flight profiles used in NIROS in PANAM. In order to model these flight profiles PraDO is used to simulate the 3D flight dynamics. Exactly the same height profile is flown with this aircraft. The output of PraDO is used in PANAM to calculate the noise produced by these profiles.

The new approach and departure contours simulated using PANAM are shown in figure 5.4.

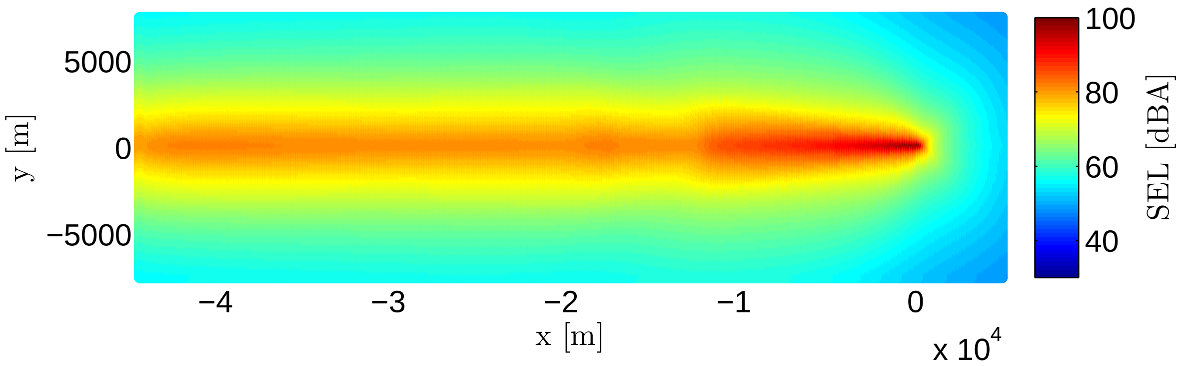

(a) Approach

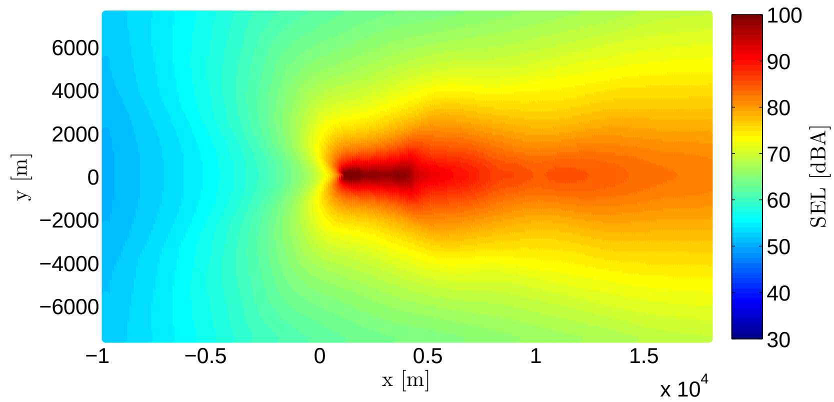

(b) Departure

Figure 5.4: A319 SEL noise contours of PANAM simulations with NIROS vertical flight profile

In figure 5.5 the approach values are given for observers directly under the flight path. The results of NIROS are also shown for comparison. It can be seen that PANAM still predicts higher values during the approach. The average difference in SEL level is around 8 dBA. After x=0 the flight path created for PANAM ends and thus these values cannot be compared. For the same flight phase (-45000 m to 0 m) the difference between NIROS and PANAM in the first simulation is around 8 dBA. Thus the overall difference between NIROS and PANAM did not change. However it can be clearly observed that at the end of the approach the predictions are closer together. This is due to the fact that the height of both simulations is equal and the thrust is of comparable magnitude.

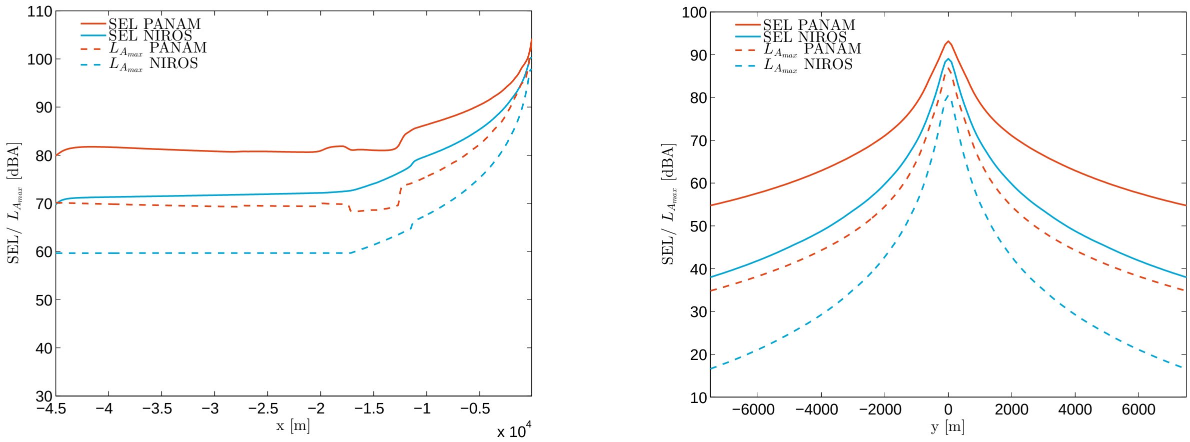

(a) Longitudinal noise directly under the flight path (b) Lateral noise at x= -3000 m

Figure 5.5: A319 approach simulations comparison NIROS and PANAM with same vertical profiles

Figure 5.6 shows the plots of thrust and velocity of both simulations. During the simulation almost the same velocity is generated in PraDO to create a good comparison. This results in almost identical velocity during the approach. The thrust needed for this procedure is much higher than the thrust calculated in NIROS. Only during the final phase (from -10 km onward) of the approach the thrust is almost the same. Just before -7 km the thrust is exactly the same. However in the plots it can be seen that there is still a gap of around 6 dBA between the SEL predictions. The difference in thrust might be one of the explanations of the noise level difference at the beginning of the approach.

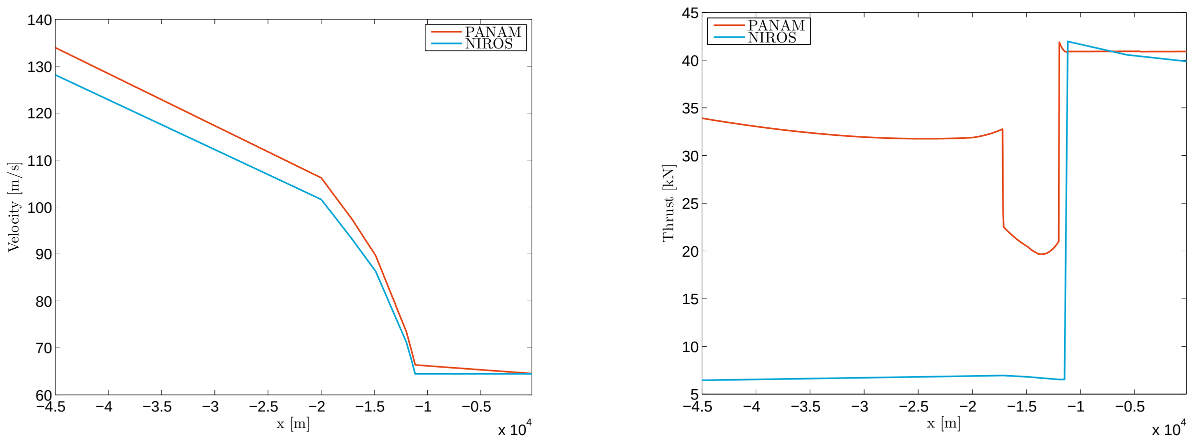

(a) Velocity (b) Thrust

Figure 5.6: A319 approach thrust and velocity comparison PANAM and NIROS

In figure 5.7 the departure noise levels are given. For the observers located directly under the flight path the difference in SEL between PANAM and NIROS is 9.2 dBA on average. Comparing this value with the level difference in the first simulations, gives a reduction of around 2 dBA. So the predictions of PANAM and NIROS are 2 dBA closer together. For both the lateral and longitudinal noise the difference increases with increasing distance to the runway.

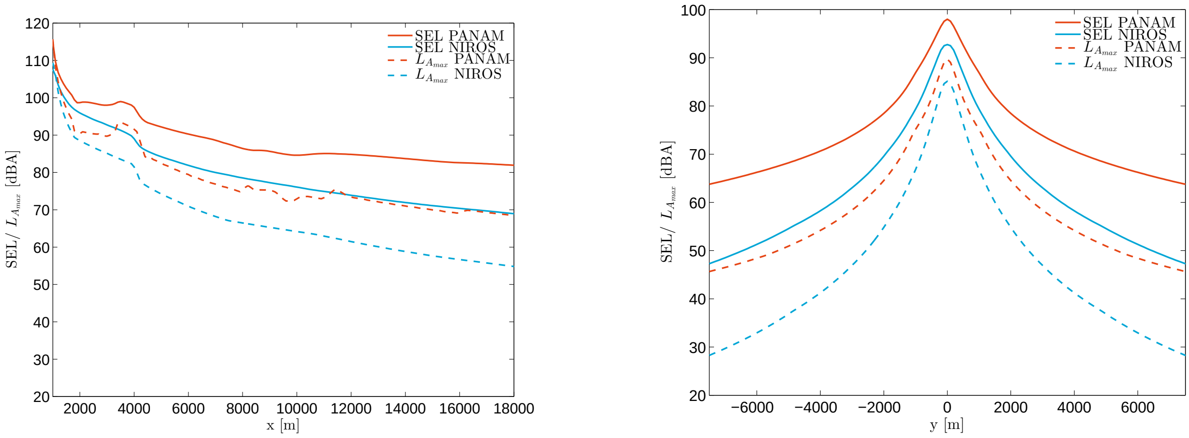

(a) Longitudinal noise directly under the flight path

(b) Lateral noise at x= 3000 m

Figure 5.7: A319 departure simulations comparison NIROS and PANAM with same vertical profiles

In figure 5.8 the velocity and thrust are plotted for the departure simulations. Again the goal was to achieve the same velocity profile as created by NIROS. However implementing this profile in PANAM created a thrust profile with many variations. It can be concluded that the thrust calculated by NIROS is very different from the thrust calculated within PraDO. Almost for all points (except the start of the manoeuvre) the used thrust in PANAM is lower than the thrust calculated in NIROS. Around 4000 m the thrust used in PANAM and NIROS is equal, however this only increase the gap between the noise predictions. So aligning the thrust will only increase the differences between PANAM and NIROS for the departure.

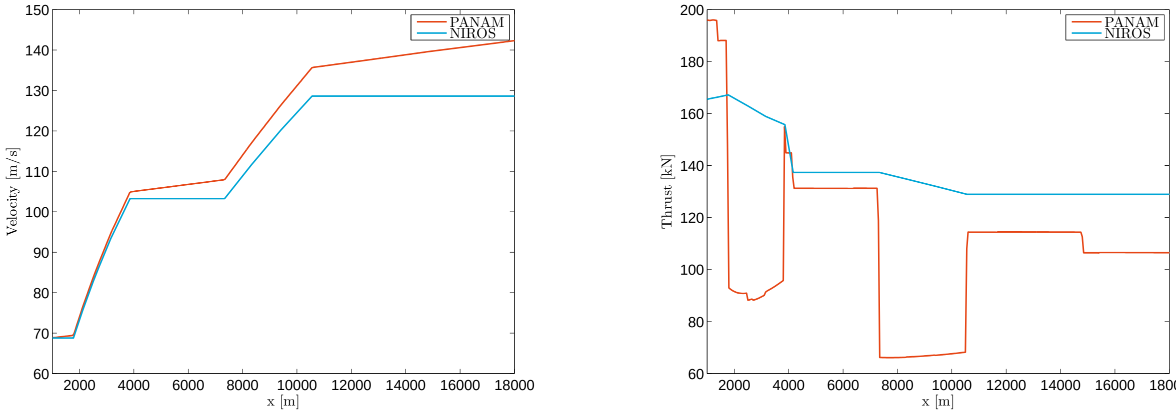

(a) Velocity

(b) Thrust

Figure 5.8: A319 departure thrust and velocity comparison PANAM and NIROS

In conclusion, simulating the vertical profile of NIROS in PANAM changes the noise predictions in PANAM. For the approach this will not change the average difference in predicted noise between PANAM and NIROS. This might be partly the result of the high thrust level needed for this profile calculated by PrADO. For the departure the difference between the two model predictions will be reduced by 2 dBA. Thus aligning the vertical flight profiles can not explain the entire offset between both model predictions.

5.2. Influence of engine differences

As described in section 4.2.1 the both models use an A319 with different engines. The engine differences can be quantified using the European Aviation Safety Agency (EASA) noise certification database[21]. This database contains noise levels of several aircraft with specific engine types. The noise is measured at three points; lateral, during the approach and during the departure. These certification points are showed in figure 5.9.

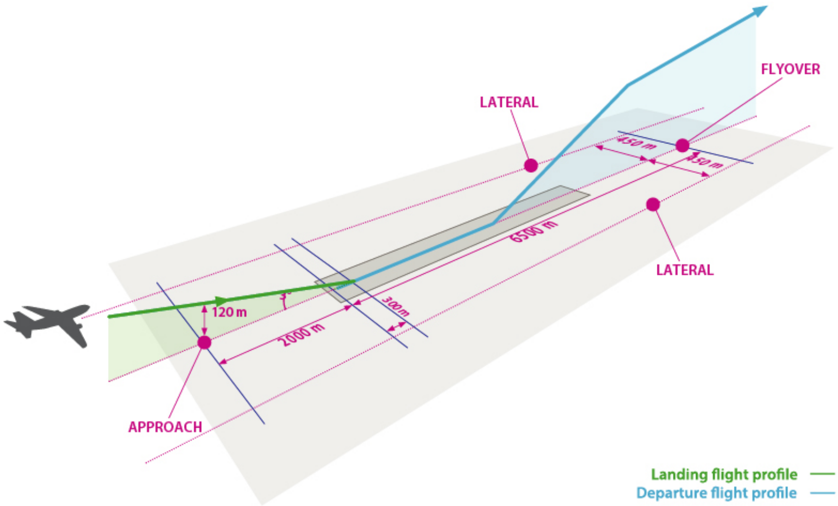

Figure 5.9: Certification points [21]

In table 5.1 the specific noise metric values for the aircraft used in NIROS (V2522-A4 engines) and PANAM (CFM 56-5A5 engines) are given. The values of the noise produced by the aircraft are close to each other. The maximum difference occurs in the lateral noise level.

Table 5.1: Certification noise A319 types [22]

	A319 with V2522-A5 engines	A319 with CFM 56-5A5 engines	Δ EPNdB
Lateral level (EPNdB)	90.9	93.6	2.7
Flyover level (EPNdB)	85.4	87.0	1.6
Approach level (EPNdB)	94.3	94.6	0.3

All values in these table are given in EPNdB which is the unit of the Effective Perceived Noise Level (EPNL). This metric is annoyance based instead of the loudness based $L_{A_{max}}$ and SEL.[32] EPNL is calculated by the time integration of the tone corrected perceived noise level (PNLT) according to equations 5.1.[45]

$$EPNL = 10\log\frac{1}{T_0}\int_{t(1)}^{t(2)} 10^{\frac{PNLT}{10}}\,dt \tag{5.1}$$

The metric EPNL is thus corrected for both spectral irregularities (by tone correction) and duration. EPNL and SEL differ mostly because of the tone correction of the EPNL. This has an influence on the predictions of early jet aircraft (high fan and turbine tones) but do not affect the aircraft used in this comparison to a great extend. For modern aircraft a constant can be used to convert EPNdB to dBA.[34] Thus the assumption can be made that the difference in EPNdB can also be used as the difference in dBA. In conclusion, the difference in engines used in the simulations can explain a difference in the noise of up to 2.7 dBA laterally.

5.3. Noise source modelling in PANAM

As concluded in the results of the simulations in section 4.4, variations in airframe configuration and/or thrust are visible in the PANAM simulations for the approach. In this section the presence of these variations are discussed in more detail. Due to the fact that PANAM predicts every noise source individually, it is possible to create noise contours of engine noise and airframe noise separately. This will help to identify which sources of noise are dominant in PANAM. This is not possible for the predictions using NIROS due to the use of NPD tables.

Figure 5.10 shows the noise contributions of the engine and airframe during the approach. The departure engine and airframe contributions are shown in figure 5.11.

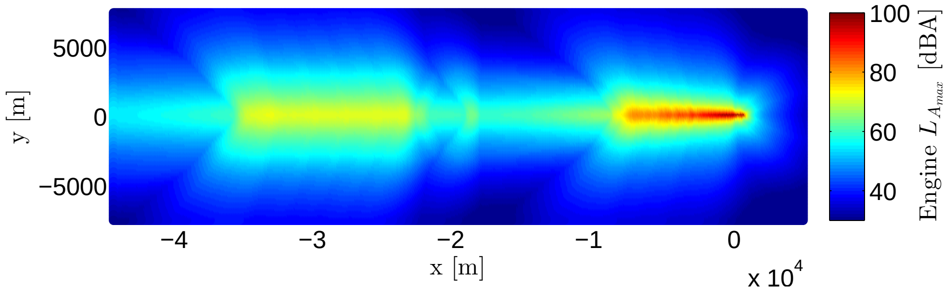

(a) $L_{A_{max}}$ engine contribution

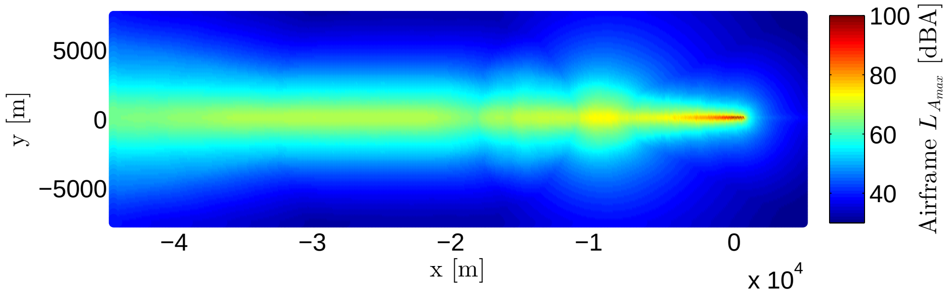

(b) $L_{A_{max}}$ airframe contribution

Figure 5.10: Component noise contributions PANAM LDLP approach

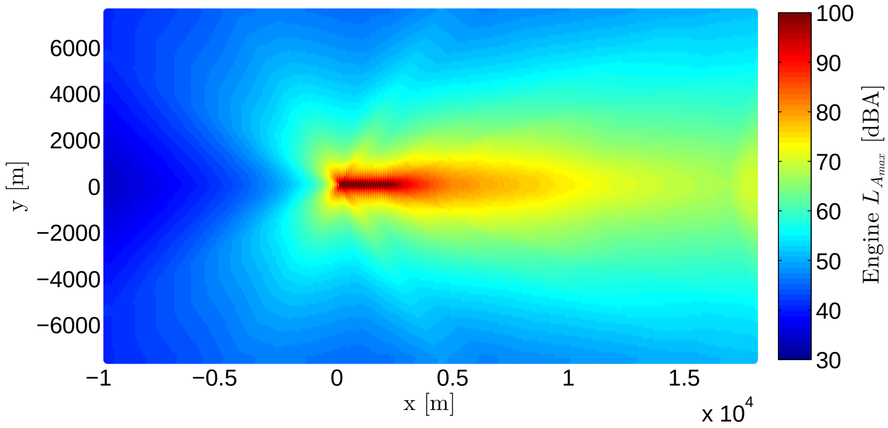

(a) $L_{A_{max}}$ engine contribution

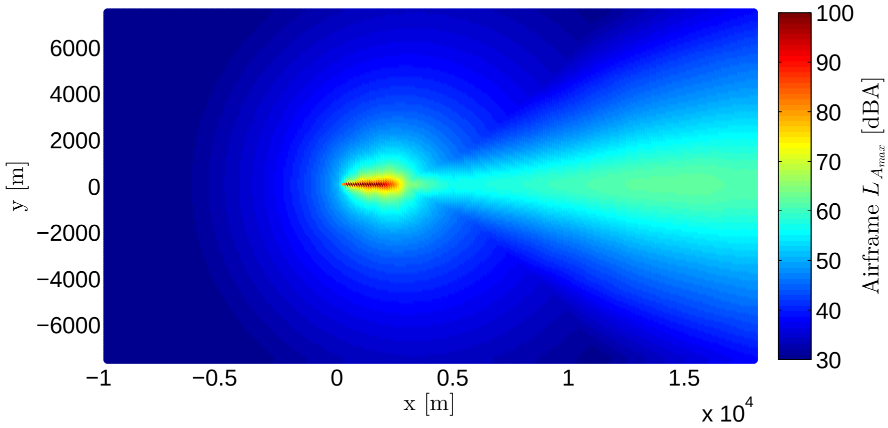

(b) $L_{A_{max}}$ airframe contribution

Figure 5.11: Component noise contributions PANAM MODATA departure

In the noise contours of the approach it can be seen that the airframe noise is dominant during the first part of the approach. Just before the landing (between -20 and -7.5 km) the airframe noise is dominant. For the departure the engine noise is clearly dominating the noise predictions. And thus airframe configuration changes can not be distinguished in this phase of flight.

The predicted noise directly under the flight path is given in figure 5.12 for the approach.

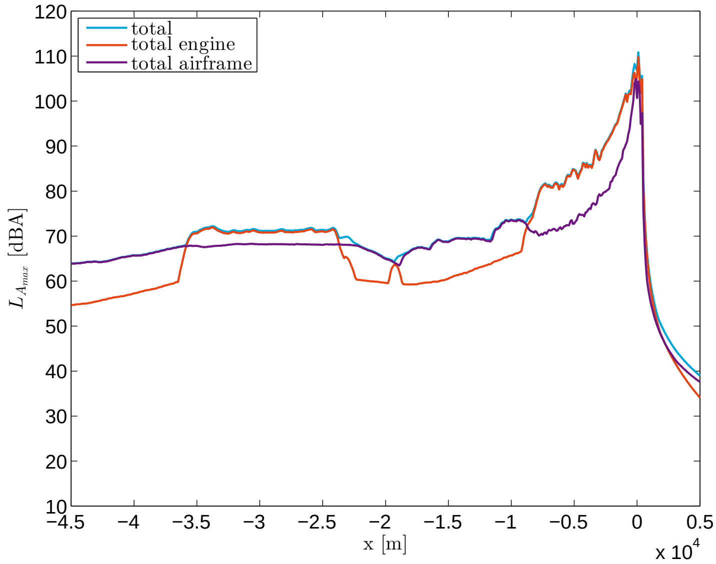

Figure 5.12: Approach airframe and engine noise directly under the flight path predicted by PANAM

It can be concluded that for certain flight segments the airframe noise is dominating and for others the engine noise. The airframe noise results from the modelling of the wings including the flaps, slats, spoilers and landing gear. These four sources can be plotted to see which has the biggest influence on the predictions during the approach. In figure 5.13 the noise per subcomponent is plotted. For the airframe noise the wing is dominating at the start of the approach. However later on, the slats and landing gear produce more noise. During the last phase of the landing (around x=0) the spoilers produce noise. The fan noise is dominating the engine noise during the entire approach.

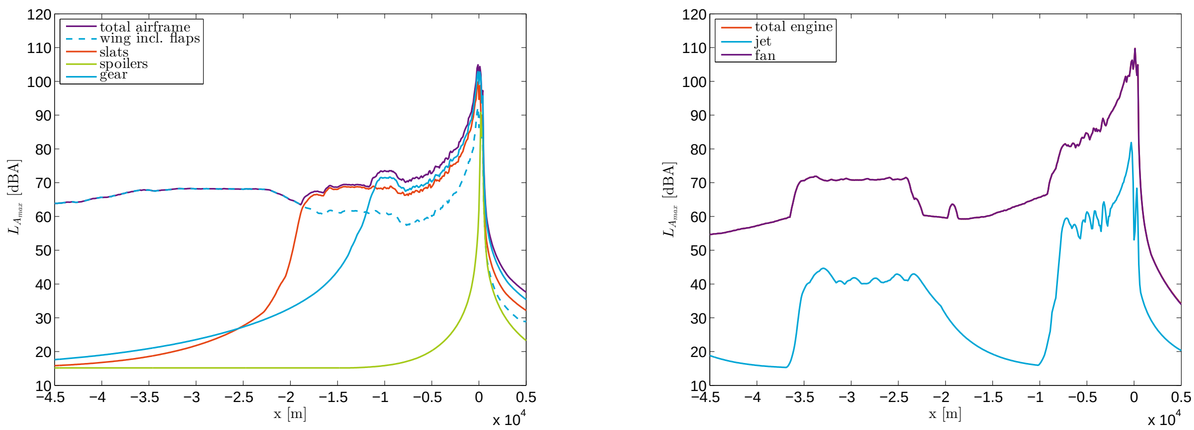

(a) Airframe noise subcomponents (b) Engine noise subcomponents

Figure 5.13: Approach subcomponents of noise prediction directly under the flight path predicted by PANAM

During the departure the engine noise is dominant. Airframe configuration changes do not affect the produced noise as discussed in section 4.2.2. The flaps and slats are not modelled in the departure simulation within PANAM due to the lack of data. In figure 5.14 the airframe and engine noise contributions during the departure are shown. During the departure the fan noise is dominant.

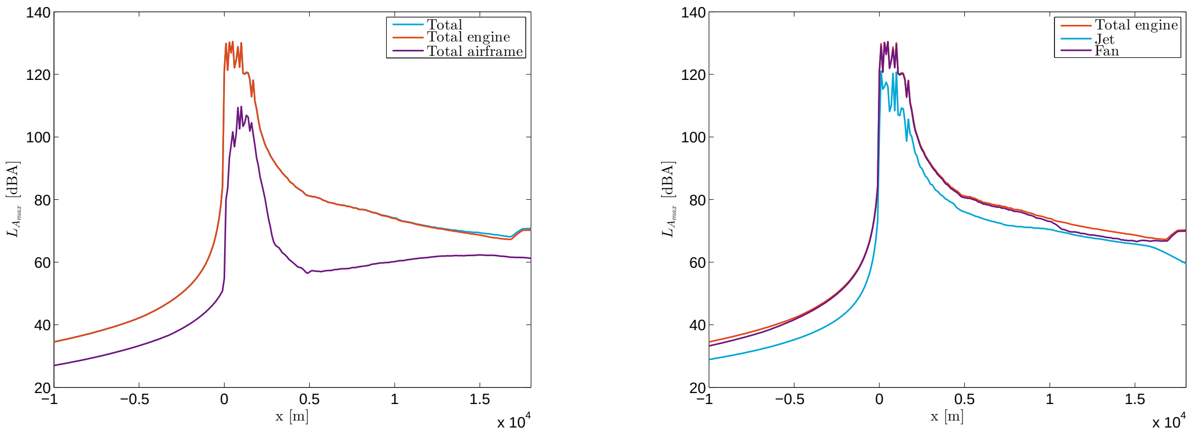

(a) Airframe and engine noise

(b) Engine noise subcomponents

Figure 5.14: Departure noise predictions directly under the flight path predicted by PANAM

So for the approach the configurations changes visible in the noise predictions are the extension of the slats and gear. During the departure the engine noise is dominant in PANAM and thus changes in the configuration will not affect the noise predictions.

5.4. Influence of ground reflection

In NIROS the ground reflection is calculated based on AIR-1751. The correction is applied with the lateral attenuation correction factor $\Lambda(\beta, l)$. This empirical relationship can be found in Appendix B. The appendix also describes the equations used for the ground reflection in PANAM using the AzB model. In figure 5.15 the ground reflection methods used in PANAM and NIROS are plotted. This graph shows the influence of ground reflection in dBA for an aircraft flying at 500 m height.

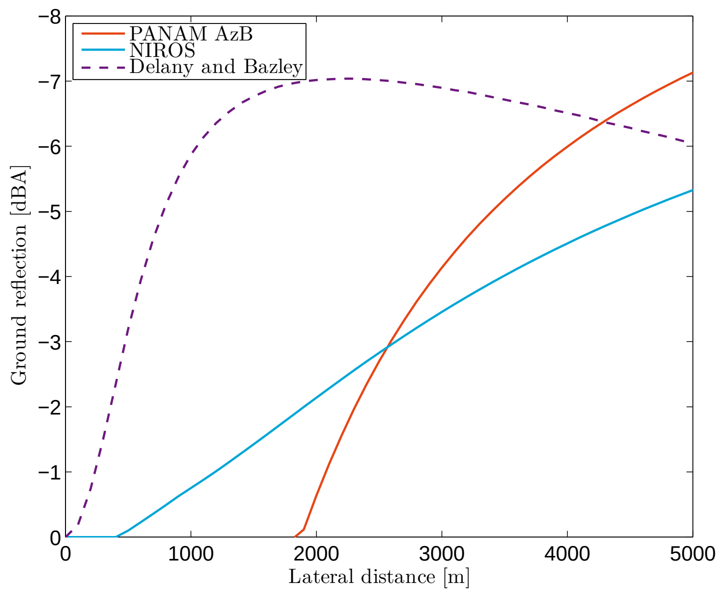

Figure 5.15: Ground reflection for the models NIROS, PANAM's AzB and Delany and Bazley for an aircraft flying at 500 m

There are variations in the used ground reflection methods. Between PANAM and NIROS this can cause differences up to 2 dBA when varying over the range of heights used in the simulations. Close to the runway NIROS predict a higher ground reflection loss. After around 2500 m lateral distance PANAM will predict a higher ground reflection loss. This means when aligning the ground reflection methods, the predictions close to the runway will be closer together. However for the predictions further away the difference in noise level will increase. In this figure also another often used method, the one described by Delany and Bazley [16], is plotted. For this method the soil type needs to be specified. In the graph a soft type of soil is used with a effective flow resistivity σ_e of 200 kPA/m^2. It can be seen that this method highly differs from the PANAM and NIROS used method. There are several other ground reflection methods and the choice of method has a large influence on the noise predictions. However for the comparison between PANAM and NIROS the ground reflection method causes differences of ± 2 dBA.

5.5. Influence of differences in the atmospheric absorption

The atmospheric absorption models used by NIROS and PANAM are different. In PANAM the atmospheric absorption is calculated using the ANSI [44] model. The SAE AIR-1845 is used to normalise the NPD tables in the ANP database. As described in chapter 3.1 the NPD tables are adjusted when the user defines other atmospheric conditions. This adjustment is according to the ARP-866A.[15] In the simulation case the reference atmospheric conditions are used and thus no adjustments have been made in NIROS.

The transmission loss A_a due to atmospheric absorption is calculated [2] as:

$$A_a = -\alpha \cdot r \tag{5.2}$$

In this equation r is the distance between the observer and source. In figure 5.16 the SAE AIR-1845 and ANSI model are plotted.

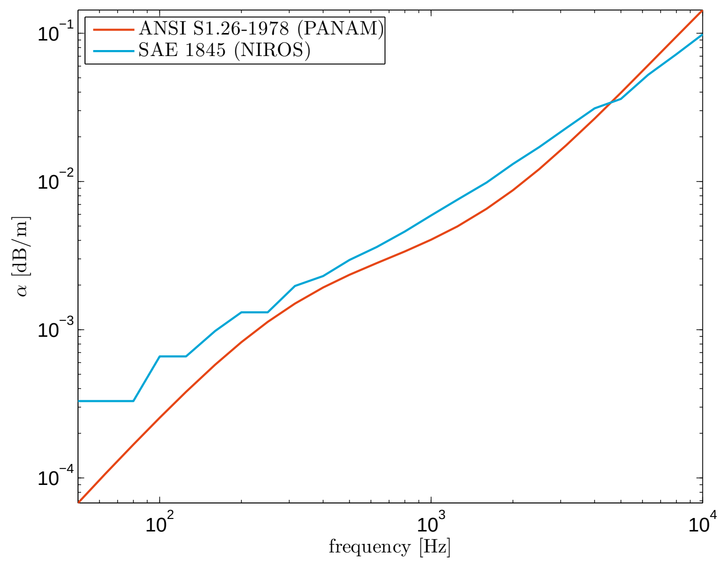

Figure 5.16: Atmospheric absorption

The graph in figure 5.16 shows that only for high frequencies the atmospheric attenuation coefficient α used in PANAM is higher than in NIROS, which will lead to a higher value of atmospheric absorption. However for the greater part of the frequency spectrum showed, NIROS accounts for a higher atmospheric absorption. The influence of the difference in atmospheric model is small. This observation is already made in several other reports.[48] [19] Using heights of a few thousand feet it can cause variations up to 4 dB.[48] However with lower heights the differences between the two models are negligible. [19]

6

Validation and discussion

This last part of the research includes the validation of the simulations. Moreover the key differences between both models will be discussed. In this chapter the first simulations of PANAM and NIROS are compared with measurement data. In section 6.1 the results of this validation are discussed. Section 6.2 will discuss the key differences resulting from this research.

6.1. Comparison with measurement data

In this section the predictions of PANAM and NIROS are compared with measurement data. In 2006 DLR executed a flyover campaign with nine approaches and landings with an A319. This data was used by Bertsch[4] to validate PANAM and is also applied in this validation. In this section two of the flights will be used to validate the results given in chapter 4. When assessing the results of this validation it should be taken into account that the validation data is acquired using the same approach and departure procedures PANAM uses. In figure 6.1 the results of the validation are shown.

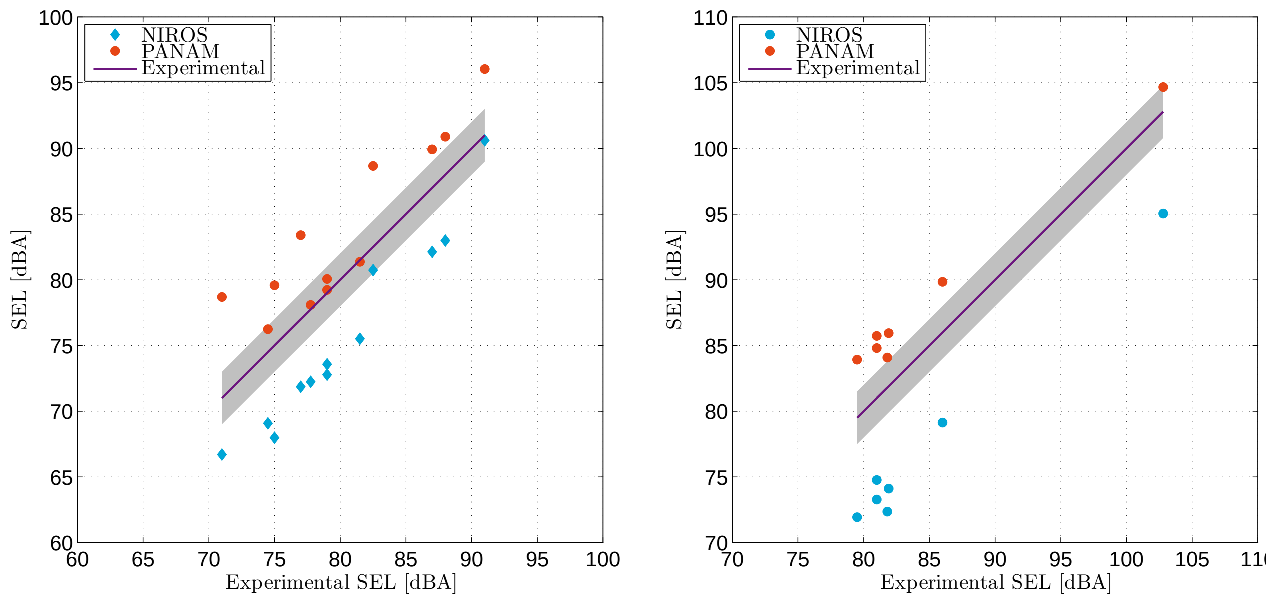

(a) Approach (b) Departure

Figure 6.1: Comparison PANAM and NIROS with microphone data

For both the approach and departure, PANAM predicts higher noise levels than measured during the experiments. NIROS predicts lower noise values. Both models follow the same trend as the experimental values and there are no outliers. For the departure NIROS predictions deviate more from the experimental values than during the approach. The figures also indicate the region of measurement uncertainty as used by Bertsch[4]. For the approach 5 points of PANAM and 2 of NIROS are within this range. This is not the case during the departure. Here all points are outside of the uncertainty range.

In figure 6.2a the microphone locations are given with respect to the approach flight path. The SEL values calculated for each location are given in 6.2b. This graph also gives the experimental values with a range(± 2 dBA) to account for uncertainty and measurement errors.

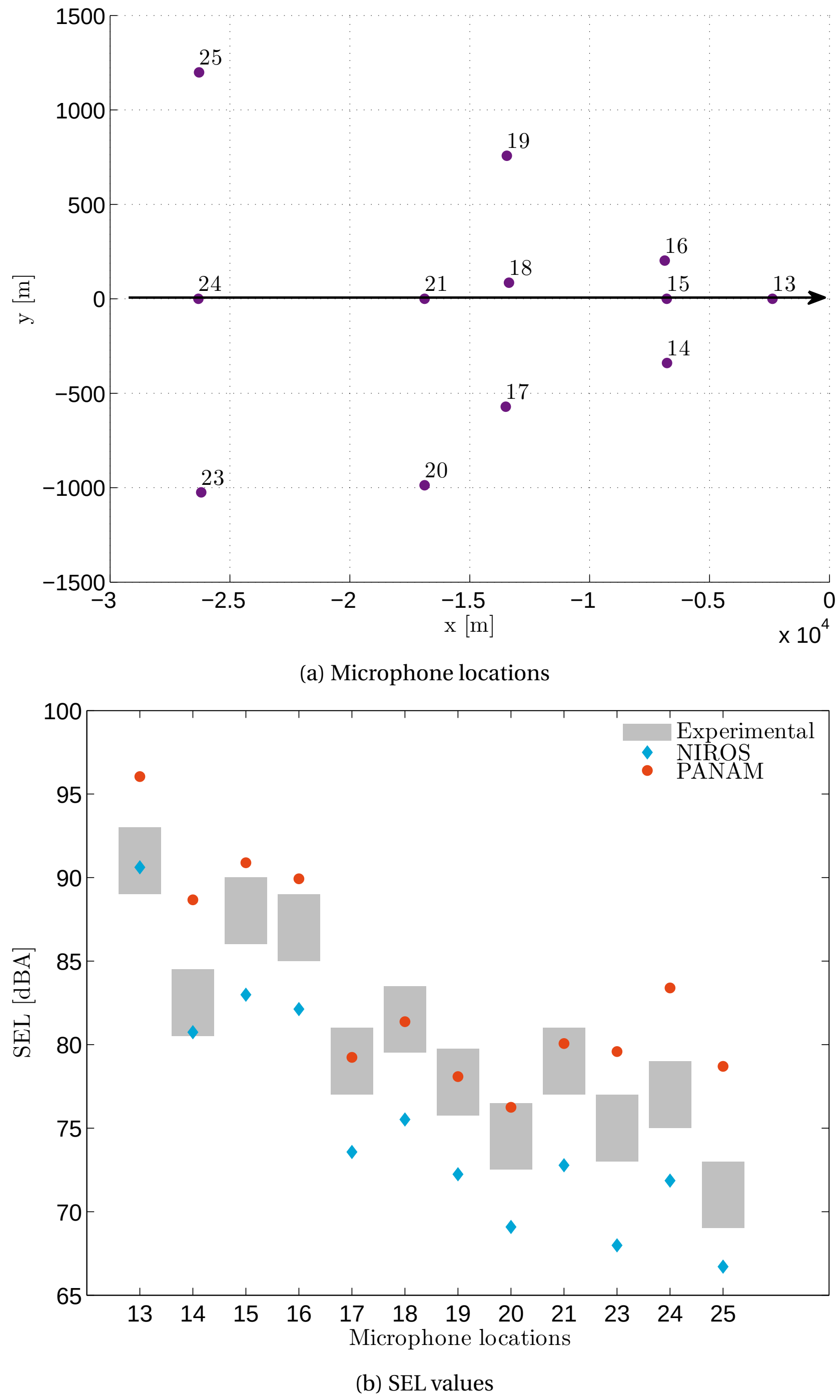

Figure 6.2: Comparison PANAM and NIROS with microphone data approach

For two points close to the runway (13 and 14) NIROS predicts noise within the experimental range. For all other points the predictions are lower than the experimental values. PANAM predicts closely to the experimental values for observers in the middle of the approach (-20km to -10km). For all other points PANAM predicts higher values for the approach.

In figure 6.3a the measurement locations for the departure are given. There are less measurement locations than during the approach. Some microphone results were corrupted. Also some locations were removed during the Parchim study because of too low incident angles with respect to the flight path. These low angle measurements have too large uncertainties due to sound propagation effects.[4]

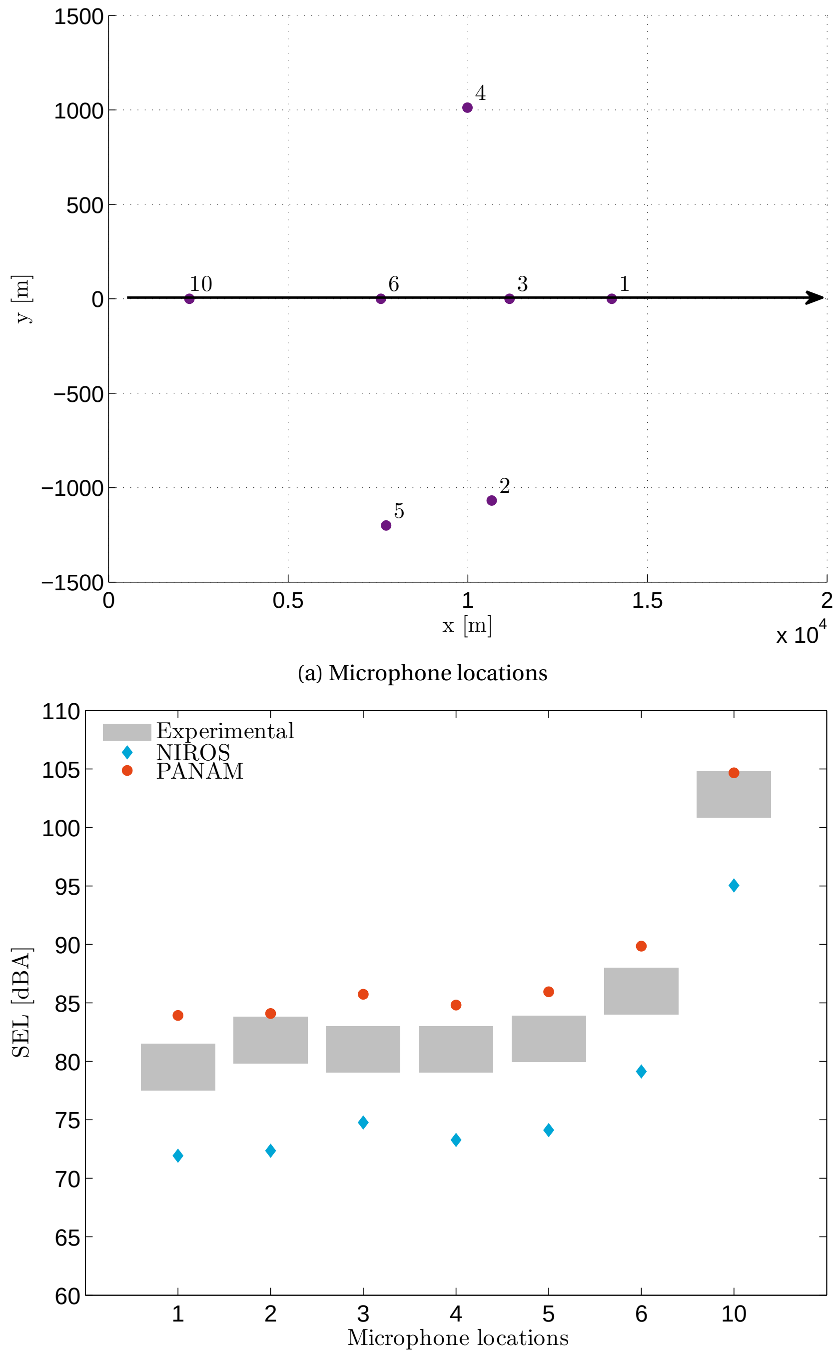

(b) SEL values

Figure 6.3: Comparison PANAM and NIROS with microphone data departure

Almost all predictions of PANAM are higher than those measured by the microphones. Only at microphone location 10 the predicted noise lies within the range. The opposite holds for the NIROS predictions; all predictions are lower than the experimental values.

Figure 6.4 shows the NIROS predictions plotted versus the PANAM predictions. Only the points used in this validations are plotted. It can be observed that all noise levels of PANAM used for this validation have higher values.

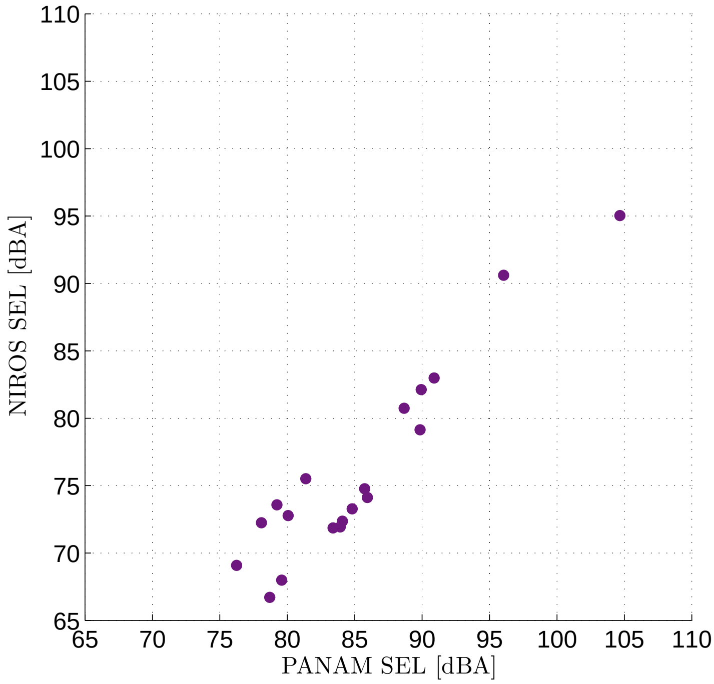

Figure 6.4: NIROS versus PANAM

In conclusion, for this test case all values predicted by NIROS and PANAM are realistic. However, comparing the data with experimental data lead to differences. PANAM predicts higher values and NIROS predicts lower values. These differences are the highest during the departure for the noise levels predicted by NIROS.

6.2. Discussion of the key differences

From the simulations of both approach and departure it was shown that higher noise levels are predicted by PANAM than NIROS. The average difference in SEL for the approach is around 7.7 dBA and for the departure 13.4 dBA. For the approach and departure these differences have a lower value when the aircraft is closer to the runway.

The trends of both model predictions are similar. However for PANAM during the approach there are more variations visible. These variations can be attributed to the difference in calculation methods of both models. The changes in configurations do not affect the noise contours in NIROS to a great extend due to the use of NPD tables. In semi-empirical models as PANAM the modelling of separate sources accounts for the change in configuration. This results in more variations in the predicted noise levels. However the biggest part of these variations are caused by the increase or decrease in thrust level. Which has a larger effect on the approach predictions in PANAM than NIROS.

During the analysis of the simulation results possible sources of these discrepancies in noise level were discussed:

Vertical flight profile differences It was not possible to create the flight profiles used in PANAM (the LDLP and MODATA) in NIROS due to the calculation methods used within NIROS. However, it was possible to calculate the predicted noise in PANAM using the flight profiles defined in the ANP database of NIROS. The change in profile did not affect the average difference in noise level between NIROS and PANAM for the approach. Using the same vertical profile in PANAM as used in NIROS reduced the noise calculated within PANAM with 2 dBA on average during the departure.

Engine differences The different engines used on both A319 aircraft can cause a difference of up to Δ 2.7 dBA laterally. The use of different engines will also cause a discrepancy during the departure of around 1.6 dBA. It will have a negligible influence on the approach noise levels.

Ground reflection method differences There are a lot of different methods to calculate the ground reflection. In PANAM as a default the AzB ground reflection method is used. In NIROS a correction factor is applied to account for ground reflection. This will have a maximum influence of ± 2 dBA on the noise predictions laterally.

Atmospheric absorption differences The different methods used for atmospheric absorption will not affect the results.

There is a huge difference in computation time between PANAM and NIROS. NIROS can calculate the noise predictions for a grid of observers within a minute. For the same predictions PANAM can take 2-6 hours. This computation time is directly related to the flight path length and number of observers. These values are of course also dependent on the computer used.

Other important differences are the accessibility of the data needed for the predictions. Within NIROS 140 aircraft can be used for predictions. For PANAM very detailed information is needed and thus a limited amount of aircraft can be assessed.

It should be noted that all results presented in this research are based on predictions of the A319. Other aircraft might cause other differences between empirical and semi-empirical noise predictions. However in this research it was not possible to access the data for other aircraft within PANAM.

7

Sensitivity analysis NIROS and possible improvements

In this chapter it is investigated which (user) inputs have an influence on the predicted noise by NIROS. This will attribute to answering the second research question regarding possible improvements of NIROS.

The user interface of NIROS makes it possible to change the atmospheric conditions for both approach and departure flights and this is discussed in section 7.1. Additionally the weight can be altered during the departure which is described in section 7.2. In section 7.3 the effect of a slight error in the input file 'procedural steps' is investigated. The influence of a small error in the input is checked with the original simulation results of NIROS (chapter 4). The noise metric which is used for this analysis is the SEL. For both the approach and departure four observer locations were chosen to execute this small sensitivity analysis. These observer locations are given in table 7.1. Finally, in section 7.4, the findings of the sensitivity will be combined with conclusions of the research in order to answer the second research question.

Table 7.1: Observer locations sensitivity analysis

	Approach			**Departure**	
No.	x (m)	y(m)	No.	x (m)	y(m)
1	-400	0	5	400	0
2	-5000	0	6	5000	0
3	-5000	2000	7	5000	2000
4	-20000	0	8	15000	0

7.1. Change in atmosphere

The user input parameters among others contain the atmospheric constants. The default option is a temperature of 15 ° C and 70 % humidity. This section describes the influences of deviations of these values. Both the temperature and humidity are increased and decreased by 20 % for the approach and departure. The results at the four observer points are given in table 7.2 and 7.3.

Table 7.2: Results change in atmospheric conditions approach, reference T=15 ° C RH=70 % humidity

	+20% influence (dBA)				**-20% influence (dBA)**			
	1	2	3	4	1	2	3	4
Humidity	0	0.03	0.2	0.09	0	0.03	0.2	0.09
Temperature	0	0.02	0.15	0.07	0	0.03	0.24	0.12

Table 7.3: Results change in atmospheric conditions departure, T=15 ° C RH=70 % humidity

	+20% influence (dBA)				**-20% influence (dBA)**			
	5	6	7	8	5	6	7	8
Humidity	0	0.05	0.17	0.15	0	0.05	0.17	0.15
Temperature	0	0.03	0.11	0.1	0	0.07	0.23	0.2

For all the locations both an increase and decrease in humidity and temperature results in a slightly higher noise levels. When the height of the aircraft increases (further away from the runway) the difference between the standard values and the new ones increases. These small increases in noise level are due to the difference in method applied. When adjusting the atmospheric conditions the ARP-866A method is used instead of the SAE AIR-1845. This slightly changes the results, even when using the standard atmospheric conditions.

The outcome of the sensitivity analysis is remarkable because normally a higher temperature leads to higher absorption rates and thus a lower SEL [2]. Checking more extreme conditions (0 ° C and 30 ° C) gives the expected theoretical outcome for temperature variations. The results are given in table 7.4. For the humidity both increasing and decreasing will lead to a small increase in noise due to the change of method. The differences in dBA are very small. It can be concluded that slightly increasing and decreasing the humidity and atmosphere has a negligible impact on the noise predictions in NIROS.

Table 7.4: Sensitivity analysis atmospheric conditions, extreme variations

	1	2	3	4
Temperature 0 ° C	0	0.05	0.39	0.19
Temperature 30 ° C	0	-0.01	-0.06	-0.04
Humidity 45 %	0	0.02	0.2	0.09
Humidity 95 %	0	0.03	0.2	0.09

7.2. Influence of weight in NIROS

Within NIROS it is possible to adjust the departure weight of the aircraft. In the simulations of chapter 4 the lowest weight is selected. However other options for the A319-131 are 131000 lb, 136500 lb, 146100 lb and 166400 lb. The influence of changing the weight can be clearly seen in figure 7.1. Here the SEL in dBA is plotted for observers directly under the flight path. In NIROS the weight can only be changed during the departure and thus will not influence the arrival noise footprint.

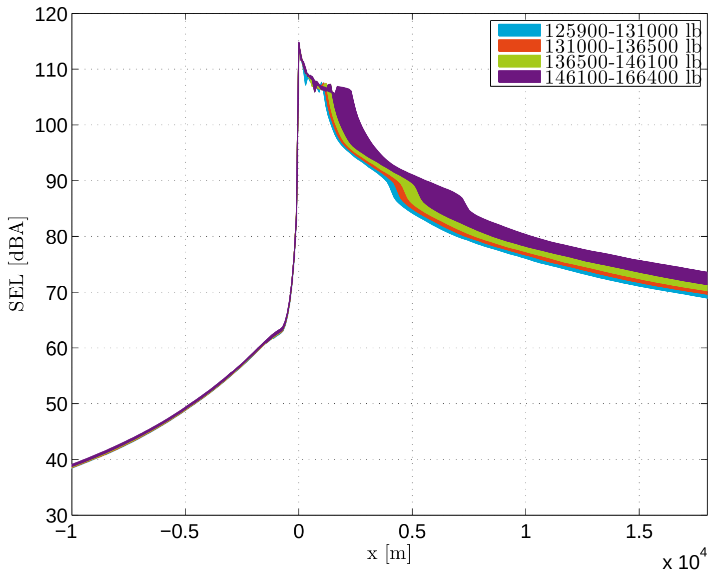

Figure 7.1: Weight variations A319-131 departure NIROS

In table 7.5 the results of the observer points of the sensitivity are shown. Generally increasing the weight results in a higher noise level. The weight increase has the least influence in the beginning of the departure procedure, so around 0 m.

Table 7.5: Results change in departure weight from reference condition 125900 lb

	Influence (dBA)			
	5	6	7	8
131000	-0.03	0.79	-0.2	0.64
136500	0.03	1.75	-0.34	1.33
146100	0.39	5.4	0.02	2.51
166400	-0.04	6.82	1.69	4.55

In figure 7.2 the changes in height, thrust and velocity are shown for the lightest and heaviest option. Due to the higher weight the aircraft needs more time to take off, and also the climb rate is lower. Moreover on average more thrust is needed for the departure. Just after the start there are some small variations due to a peak in the thrust. The velocity profiles of the different weight simulations are all comparable. However heavier aircraft take more time to accelerate to the same velocity. The result of these changed parameters is the increase in noise levels for an observer on the ground. Due to the lower height and increased thrust level the noise level of the heavy option decreases later than the lower weight option. In conclusions, choosing heavier aircraft will increase the noise level substantially.

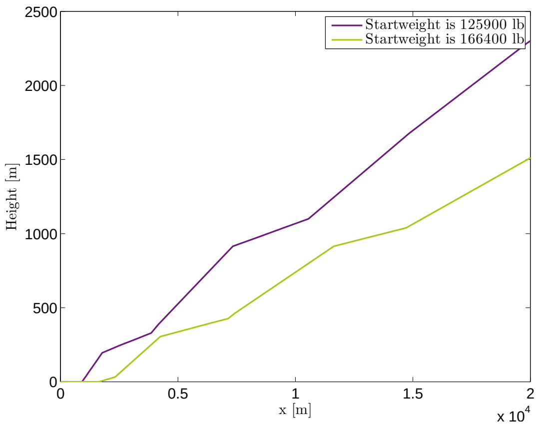

(a) Height

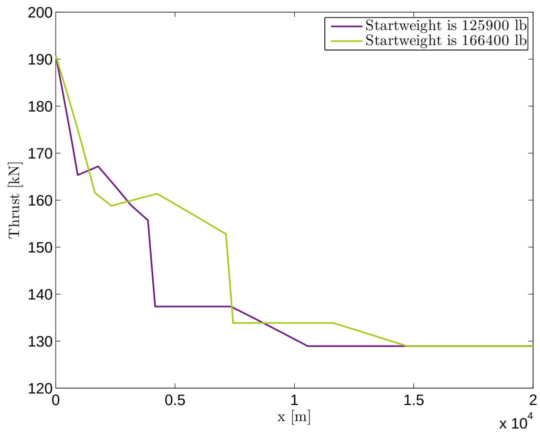

(b) Thrust

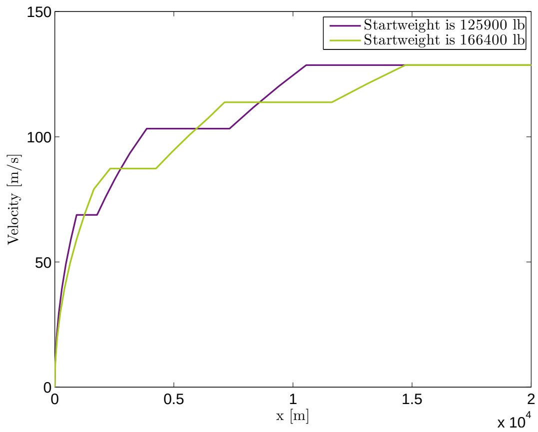

(c) Velocity

Figure 7.2: Differences in calculated parameters NIROS

7.3. Procedural steps

The input file 'Procedural steps' determines the flight profile in NIROS. The approach and departure procedural steps are given in tables 7.6 and 7.7 . The variables in the approach and departure tables differ due to the different formulas used to calculate the profiles originating the ECAC documentation [15].

The purpose of this small sensitivity analysis is to see if a small error in the variables defined in the procedural steps influences the perceived noise calculated by NIROS. The variables altitude, velocity (CAS), decent angle (approach) and rate of climb (departure) are increased and decreased by 10 %. For both manoeuvres the flap settings are also changed. The approach has more variables such as the touchdown roll and distances however these variables will only lengthen certain steps. For each manoeuvre four observer locations were selected for the sensitivity analysis. These locations are given in table 7.1.

Table 7.6: STANDARD NIROS arrival procedural steps A319-131

	Flap ID	**Start altitude (ft)**	**Start CAS (kt)**	**Descent angle (°)**	**Touchdown roll (ft)**	**Distance (ft)**	**Start thrust (%)**
Descend-Idle		6000	250	3.1			
Level-Idle		3000	250			19940.9	
Level-Idle		3000	197.5			4813	
Descend-Idle		3000	181.4	3			
Descend-Idle		2610	167.7	3			
Descend-Idle		2114	138.4	3			
Descend	Full D	1971	125.3	3			
Descend	Full D	50	125.3	3			
Land	Full D				152.3		
Decelerate			122.3			1370.6	40
Decelerate			30			0	10

Table 7.7: STANDARD NIROS departure procedural steps A319-131

	Thrust rating	**Flap ID**	**End point altitude (ft)**	**Rate of climb (ft/min)**	**End point CAS (kt)**
Takeoff	MaxTakeoff	1+F			
Climb	MaxTakeoff	1+F	1000		
Accelerate	MaxTakeoff	1+F		1042.6	181.6
Accelerate	MaxTakeoff	1		1177.5	200.7
Climb	MaxClimb	ZERO	3000		
Accelerate	MaxClimb	ZERO		1320.8	250
Climb	MaxClimb	ZERO	5500		
Climb	MaxClimb	ZERO	7500		
Climb	MaxClimb	ZERO	10000		

In table 7.8 the results of the change in the approach procedural steps of altitude, CAS and descent angle are given.

Table 7.8: Sensitivity analysis approach procedural steps A319-131

	+10% influence (dBA)				**-10% influence (dBA)**			
	1	2	3	4	1	2	3	4
Altitude	0	0	0	-0.83	0	0	0	0.96
CAS	-0.34	-0.39	-0.4	-0.42	0.54	0.49	0.47	0.45
Descent angle	-0.76	-0.88	0.28	-0.01	0.82	0.96	-0.33	0.06

All variables have a small impact. The most surprising effect is the impact due to the increase and decrease in CAS. Increasing the CAS lowers the noise level and decreasing the CAS increases the noise level. This is different than expected because during the approach the airframe noise is often dominating. Increasing the speed of the aircraft thus normally leads to higher noise values. This is not the case in the predictions of NIROS. Due to the predefined equation in the ECAC documentation[15] for velocity for the landing segment the aircraft is forced to achieve a certain velocity (equation 7.1 [15]) at the begin of the segment.

$$CAS \approx D \cdot \sqrt(W) \tag{7.1}$$

This velocity is calculated using the landing weight W and the flap coefficient D $(kt/\sqrt{lbf})$. Consequently the aircraft with the lowered CAS is forced to increase the thrust leading to a higher noise level. After the begin of the segment, the aircraft is again forced to achieve the 10 percent lower CAS as given in the procedural steps and thus the reverse thrust is increased. The altitude has only an effect on the furthest point (No. 4). Changing the start altitude only changes the level-idle steps. Increasing the altitude lowers the noise and decreasing the altitude increases the noise. This behaviour is expected. Increasing the descent angle generally leads to a lower noise. However when looking at the height of the flight profile the descent angle is not increased. The parameter which changes is the thrust; the thrust decreases which lowers the noise. Using the formulas out of the ECAC documentation forces the aircraft to use a descent angle of 3 °. This descent angle can be only changed when also using another level step in the procedural steps. So increasing or decreasing the descent angle only affects the thrust.

The variable flap ID, which is the flap setting, can also be changed in the procedural steps. There are multiple options such as 1_A, 2 _D, 2_U and 3_D. However the only realistic alternative of the full deployment (Full D) during the approach is 3_D [46]. Full deployment means 40 ° and with 3_D the extension of the flaps is somewhat lower. The results of the lower flap deflection are showed in table 7.9. Lowering the flap and slat deflection lowers the noise predictions only close to the runway. This is expected due to the fact that the flaps are only extended in the final phase of the approach.

Table 7.9: Sensitivity analysis flaps procedural steps approach A319-131

	Influence (dBA)			
	1	2	3	4
Flaps	-0.83	-0.62	-0.44	0

Table 7.10 shows the results of the variations in altitude, rate of climb and CAS in the procedural steps of the departure. The 10 % increase and decrease of the variables altitude and rate of climb do not change the outcome considerably. These changes in noise are of negligible magnitude. The increase in altitude leads to a higher thrust in NIROS. This counteracts the effect of the higher altitude and as a result the received noise at the observer location does not change. This also holds for the increase in rate of climb. Only the increase and decrease in CAS has an influence on the outcome. Due to the increase of the CAS the accelerations sections become longer which have an effect on the perceived noise.

Table 7.10: Sensitivity analysis departure procedural steps A319-131

	10% increase influence (dBA)				**10% decrease influence (dBA)**			
	5	6	7	8	5	6	7	8
Altitude	0	0.04	-0.09	0.03	0	0.02	-0.09	0.02
Rate of climb	0	-0.03	0.11	-0.01	0	0.02	-0.09	0.02
CAS	0	1.3	-0.51	0.14	0	-0.97	0.67	0.07

In the procedural steps of the departure the flaps settings can be changed. For the A319-131 the settings possible are 1+F, 1 or ZERO. In the procedural steps the flap settings can only be increased not lowered. If a lower setting than 1+F is chosen for the first steps (take-off and climb) NIROS will produce an error message. However it is possible to increase the flap setting of the fourth till last procedural step. Surprisingly this has an effect on the perceived noise as can be seen in table 7.11. During the departure often the engine noise is dominating and the flaps do not influence the predicted noise. The effect is the highest at observer location 4, so the furthest from the runway. However it should be noted that extended flaps at that moment in the flight procedure is not a realistic scenario.

For the departure it is also possible to select an entire different procedure, the ICAO A. This procedure is different from the STANDARD one as can be seen in table 7.12. The beginning of the departure has more acceleration segments when comparing it with table 7.7. The simulated aircraft using the ICAO A procedure gains more height in the begin of the procedure resulting in less noise. Moreover the STANDARD procedure requires a higher thrust at the start of the flight procedure. At 15000 m the STANDARD profile has a higher altitude and thus the ICAO A procedure produces more noise. Both profiles have the same thrust at this point in flight.

In conclusion all three variables affect the noise predictions of the approach slightly (max 1 dBA). During the departure the CAS has the largest effect on the output. For both manoeuvres a change in flap setting will influence the predicted noise.

Table 7.11: Flaps and ICAO A departure sensitivity analysis A319-131

	Influence (dBA)			
	5	6	7	8
Flaps	0	0.29	-0.06	1.03
ICAO A	0	-1.69	0.95	1.21

Table 7.12: ICAO A departure procedural steps A319-131

	Thrust rating	**Flap ID**	**End point altitude (ft)**	**Rate of climb (ft/min)**	**End point CAS (kt)**
Takeoff	MaxTakeoff	1+F			
Climb	MaxTakeoff	1+F	1500		
Climb	MaxClimb	1+F	3000		
Accelerate	MaxClimb	1+F		822.7	181.4
Accelerate	MaxClimb	1		972.3	196.5
Accelerate	MaxClimb	ZERO		1162.8	223.8
Accelerate	MaxClimb	ZERO		1374.2	250
Climb	MaxClimb	ZERO	5500		
Climb	MaxClimb	ZERO	7500		
Climb	MaxClimb	ZERO	10000		

7.4. Possible improvements of NIROS

The second research question is to propose possible improvements for NIROS when comparing this model with PANAM. Based on the simulations, the results of the sensitivity analysis and the validation some recommendations can be given in order to improve or broaden the application of NIROS.

The most important conclusions from the sensitivity results are:

- The aircraft weight has the biggest influence on the departure noise. Increasing the weight can cause an increase of up to 7 dBA.
- Changing the temperature and humidity have a negligible effect on the simulation results.
- Slightly changing the parameters in the procedural steps of the approach have an influence of maximal ± 1 dBA
- For the departure only the change in CAS affects the noise predictions with a maximum of ± 1 dBA
- The change of procedure to ICAO A(only possible for the departure) has an effect of ± 2 dBA

From the validation it can be concluded that the approach and departure predictions are lower than the microphone results for the flight path used. For the departure the points predicted by NIROS are all outside of the uncertainty bound. This might be related to the flight profile used.

When comparing NIROS with PANAM and reviewing all simulation results some possible modifications of NIROS could be proposed. The simulations are only based on the A319. More research needs to be executed to justify these modifications.

Including more flight profiles in NIROS For the approach there is just one flight procedure defined for the A319 in NIROS. This vertical profile is not the most realistic one and will be changed in the coming years.[15] More flexibility in flight profile will extend the application of NIROS. In the sensitivity analysis it could be seen that changing the departure route to the ICAO A procedure has an influence on the predicted noise. Thus it is important to use the vertical profiles used during operations for noise predictions. Including more vertical profiles will create more flexibility within NIROS.

Implementation of multiple ground reflection methods and/or free field predictions Within PANAM there is more flexibility in the ground reflection methods. This is not the case for NIROS. It is also not possible to exclude the correction in order to simulate free field predictions. Including more ground reflection correction methods will make it possible to calculate the influence of different surfaces (soft or hard soil) on the predicted noise. This might broaden the usability of the predictions of NIROS.

Correction factor for slat and gear extension and thrust increase/decrease for approach In PANAM a steep change in thrust was clearly visible laterally during the approach. This is not the case in predictions of NIROS. Moreover the extension of the slats and gear increased the predicted noise during this manoeuvre. If this is also the case when predicting the noise of other aircraft, a correction factor can be created to include these effects in the contours.

8 Conclusions and recommendations

The research aim was to compare the noise predictions of empirical and semi-empirical noise prediction models and to assess the applicability and use of these models. Two research questions were constructed at the beginning of this research:

1. What are the major differences between empirical noise prediction and semi-empirical noise prediction models when predicting aircraft noise?

2. What are possible improvements of the empirical noise model NIROS based on the comparison with the more physics-based model PANAM?

In this chapter first the conclusions resulting from this research are described in section 8.1. After this the recommendations for future work are given in section 8.2.

8.1. Conclusions

To get a better understanding of the methods used in both models, literature on the subject was consulted. Moreover the documentation of PANAM and NIROS and the source code of NIROS were reviewed. Three major difference were found during this part of the research:

- Use of NPD tables in empirical noise modelling and noise source modelling in semi-empirical noise models.
- Differences in noise propagation methods applied for ground reflection and atmospheric absorption
- Differences in the construction of the flight path

A simulation case was constructed to examine the differences in the predictions of both models. In PANAM and NIROS an A319 was used to simulate the noise for observers located on the ground. The results of the simulations showed higher noise levels in PANAM than in NIROS. The trend of the noise levels at closely spaced observer positions directly underneath the flight path was comparable. In PANAM more variations were visible due to the separate modelling of the noise sources and the type of data used in this model. Some factors which can explain these results were analysed. The difference in flight path and the applied ground reflection method had the biggest influence on the simulation results. Validating the simulations with measurements showed that PANAM seems to overestimate the noise and NIROS underestimate the noise.

Recommendations for possible improvements of NIROS were given. Including more vertical flight profiles in NIROS will increase the flexibility of the model. Moreover it would be interesting to implement more methods for ground reflection to include the effects of different types of soil. Also correction factors for steep thrust increase/decrease and slat and gear extension might improve NIROS.

In conclusion semi-empirical models such as PANAM are more flexible. Different flight paths can be simulated and sound propagation methods can be adjusted. However the use of this kind of models is not yet a possibility for the air navigation services. Semi-empirical models such as PANAM are made to assess the noise generated by flyovers of a single aircraft. These type of models are not designed to assess the noise predictions of many aircraft over long time periods. The air navigation services use noise predictions models for hundreds of these manoeuvres and it should be possible to calculate multiple types of aircraft.

The simulations results show that all the noise values predicted by NIROS are lower than the experimental (measured) values. However, to further assess the discrepancies more data is needed. This conclusion is based on the A319 aircraft simulation only. When the results found in this research are valid for multiple aircraft, the model should be adjusted. These predictions are important for the assessment of noise pollution on the community and thus have a large influence.

8.2. Recommendations for future work

Although the goal to construct a first comparison between empirical and semi-empirical models is achieved and the research questions have been answered, some recommendations can be made for future work.

- During this research one simulation case is executed. Due to the lack of accessible information needed for the semi-empirical model PANAM it was not possible to compare multiple aircraft. For future work it would be recommended to compare simulations of different aircraft types. This will show if there is always an offset present between the predictions of the two types of models. However it should be noted that a one-to-one comparison (same engines and flight path) of the models is not feasible due to the difference in methods of both models.

- In the validation two measurement sets were used, with a total of 19 measurement points. This is a relatively low number of measurements. More validation data, and more exact levels, would better support the conclusions. Using more measurement data will make it possible to check if the conclusions presented in this research will be valid in general.

- In this research two representative models are used to compare empirical and semi-empirical models. There are more models like INM [25](empirical model) or ANoPP2 [40] (semi-empirical model) which are used widely for the prediction of aircraft noise. It would be interesting to see if the differences found in this research will also hold for the noise predictions of these models.

Bibliography

[1] Airbus. Airbus a319 - dimensions and key data. `http://www.airbus.com/aircraftfamilies/passengeraircraft/a320family/a319/specifications/`. Accessed on 01/07/2016.

[2] M. Arntzen. Aircraft noise calculation and synthesis in a non-standard atmosphere. PhD dissertation TU Delft, 2014.

[3] M. Arntzen and D. Simons. Modeling and synthesis of aircraft flyover noise. Applied Acoustics 84(2014) p.99-106, 2013.

[4] L. Bertsch. Noise prediction within conceptual aircraft design. DLR, 2013.

[5] L. Bertsch. The parametric aircraft noise analysis module(panam) technical manual & user handbook. DLR, 2014.

[6] L. Bertsch, Sebastien Guerin, Gertjan Looye, and Michael Pott-pollenske. The parametric aircraft noise analysis module - status overview and recent applications. 17th AIAA/CEAS Aeroacoustic Conference, 2011.

[7] L. Bertsch, W. Heinze, and M. Lummer et al. Application of an aircraft design-to-noise simulation process. American Institute of Aeronautics and Astronautics, 2014.

[8] L. Bertsch, D.G. Simons, and M. Snellen. Aircraft noise: The major sources, modelling capabilities, and reduction possibilities. DLR, 2015.

[9] D. J. Bodony and S. K. Lele. Generation of low frequency sound in turbulent jets. 11th AIAA/CEAS Aeroacoustic Conference 23-25 May 2005 Monterey California, 2005.

[10] R. Bütikofer. Concepts of aircraft noise calculations. Acta Acustica united with Acustica Vol, 93 p. 253-262, 2007.

[11] R. Bütikofer and G. Licitra. Noise mapping in the eu: Models and procedures - airport noise. CRC Press p145-148, 2013.

[12] W. Heinze C. Werner-Westphal and P. Horst. Multidisciplinary integrated preliminary design applied to unconventional aircraft configurations. Journal of aircraft Vol. 45, No. 2, 2008.

[13] D. Casalino, F. Diozzi, and R. Sannino. Aircraft noise reduction technologies: A bibliographic review. Aerospace Science and Technology vol. 12 p.1-17, 2008.

[14] European Civil Aviation Conference. ECAC.CEAC Doc 29 3rd edition; report on standard method of computing noise contours around civil airports, volume 1, 2005.

[15] European Civil Aviation Conference. ECAC.CEAC Doc 29 3rd edition; report on standard method of computing noise contours around civil airports, volume 2, 2005.

[16] M.E. Delaney and E.N. Bazly. Acoustical properties of fibrous absorbent materials. Applied Acoustics, 3(2), 105-116, 1970.

[17] Arbeitsgruppe 'Novellierung der AzB'. Anleitung zur berechnung von larmschutzbereichen (azb). Bundesanzeiger Nr. 195a, 2007.

[18] W. Dobrzynski. Almost 40 years of airframe noise research: What did we achieve? Journal of Aircraft vol. 47 issue 2 p. 353-367, 2010.

[19] J. Gulding D.W. Forsyth and J. Dipardo. Review of intergrated noise model (inm). NASA, 2003.

[20] EASA. Icao aircraft engine emissions databank. http://www.easa.europa.eu/document-library/icao-aircraft-engine-emissions-databank, . Accessed on 05/07/2016.

[21] EASA. Noise certification points. http://www.easa.europa.eu/eaer/topics/technology-and-design/figures-and-tables, . Accessed on 13/07/2016.

[22] EASA. Easa approved noise levels. http://www.easa.europa.eu/document-library/noise-type-certificates-approved-noise-levels, . Accessed on 05/07/2016.

[23] E. Envia, D.L. Tweedt, D.M. Elliott R.P. Woodward, E.B. Fite, C.E. Hughes, G.G. Podboy, and D.L. Sutliff. An assessment of current fan noise prediction capability. 14th Aeroacoustics Conference AIAA/CEAS, 2008.

[24] F. Farassat and J. Casper. Towards an airframe noise prediction methodology: Survey of current approaches. 44th AIAA Aerospace Sciences Meeting and Exhibit p.210, 2006.

[25] A. Filippone. Aircraft noise prediction. Progress in Aerospace Sciences vol. 68 p.27-63, 2014.

[26] A. Filippone and L. Bertsch. Comparison of aircraft noise models with flyover data. Journal of Aircraft Vol. 51 No. 3, 2014.

[27] M.R. Fink. Airframe noise prediction method. Final rept. Jun 1976-Apr 1977, 1977.

[28] D. Gély and J. Delfs. Aeroacoustic installation effects on transport aircraft research at onera and dlr. Presentation published by DLR and Onera.

[29] Y.P. Guo, K.J. Yamamoto, and R.W. Stoker. Component-based emperical model for high-lift system noise prediction. Journal of aircraft vol. 40 no.5, 2003.

[30] M. F. Heidmann. Interim prediction method for fan and compressor source noise. NASA Technical Memorandum X-71763, 1979.

[31] L. S. Hultgren. A comparison of combustor-noise models. NASA, 2012.

[32] A. Depitre ICAO. Noise certification workshop:epndb metric. presentation Bangkok, 6-7 november, 2006.

[33] U. Isermann and B. Vogelsang. Azb and ecac doc. 29- two best-practice european aircraft noise prediction models. Noise control engineering journal, 2010.

[34] K. Jones and R. Cadoux. Ercd report 0904: Metrics for aircraft noise. Civil Aviation Authority, 2014.

[35] B. A. Janardan K. B. Kontos and P. R. Gliebe. Improved nasa-anopp noise prediction computer code for advanced subsonic propulsion systems volume 1 and 2. NASA Contractor report, 1996.

[36] W. Krebs. Sound source data for aircraft noise simulation. Acta Acustica united with Acustica Vol, 90 p. 91-100, 2004.

[37] J. Kurzke. Gasturb 9 users manual; a program to calculate design and off-design performance of gas turbines. www.gasturb.de, 2001.

[38] M. J. Lighthill. On sound generated aerodynamically: I. general theory. Department of Mathematics, The University, Manchester, 1951.

[39] G.M. Lilley. Jet noise classical theory and experiments. Aeroacoustics of flight vehicles: theory and practice. Vol. 1: Noise sources, 1991.

[40] L. Loper and C. Burely. Design of the next generation aircraft noise prediction program: Anopp2. AIAA/CEAS aeroacoustic conference 2011, 2011.

[41] A. McAlpine and M.J. Fisher. On the prediction of 'buzz-saw' noise in aero-engine inlet ducts. Journal of Sound and Vibration vol. 248 p. 123-149, 2001.

[42] P. Morris and F. Farassat. Acoustic analogy and alternative theories for jet noise prediction. AIAA journal vol. 40 issue 4 p.671-680, 2002.

[43] W. Neise. Larmoptimierte an- und abflugverfahren (lanab); zusammenfassender schlussbericht. Bundesministerium fur Wirtschaft und Technologie, 2007.

[44] Acoustical Society of America. Method for the calculation of the absorption of sound by the atmosphere. ANSI S1.26-1978, 1995.

[45] International Civil Aviation Organization. Environmental protection annex 16 volume 1 aircraft noise. ICAO, 2014.

[46] E. Parks. Airbus notes; training notes for a319/a320/a321. online, 2016.

[47] S. Pietrzko and R. Bütikofer. Flula - swiss aircraft noise prediction program. Acoustics 2002- Innovation in Acoustics and Vibration - Annual Conference of the Autralian Acoustical Society, 2002.

[48] K. J. Plotkin. Analysis of acousti modeling and sound propagation in aircraft noise prediction. NASA, 2006.

[49] G.J.J. Ruijgrok. Elements of aviation acoustics. Delft University Press, 1993.

[50] G.J.J. Ruijgrok. Elements of airplane performance. VSSD, 2009.

[51] M.J.T. Smith. Aircraft noise. Cambridge University Press, 1989.

[52] J. R. Stone. Interim prediction method for jet noise. NASA TM X-71618, 1974.

[53] C.K.W. Tam, K. Viswanathan, K.K. Ahuja, and J. Panda. The sources of jet noise: experimental evidence. J. Fluid Mech. vol. 615 p. 253-292 Cambridge University Press, 2008.

[54] K. W. Tam and L. Auriault. Jet mixing noise from fine-scale turbulence. AIAA journal Vol. 37, No. 2, 1999.

A

Inputs PANAM

Table A.1: Inputs PANAM part 1

Aircraft geometry	
Wing, flap, slat	Sweep angle
	Airfoil mean chord length
	Flap mean chord length
	Slat mean chord length
	Element wide
	Installation angle
Spoiler dimensions	
Tail dimensions	
Landing gear dimensions	Extended length
	Wheel diameter
	Number of axles
Number of engines	
Wing loading	Start and landing
Observer array	x, y, z location of every observer
Engine parameters	
	Number of fan rotors & stators
	Design Mach number of fan tip
	Rotor stator spacing
	Fan hub to tip ratio
	Fan radius
	Max fan RMP
	Max RMP 2nd shaft
	Fan blade chord length
	Lining intake and bypass length

Table A.2: Inputs PANAM part 2

Engine stage information	
	Mach number
	Thrust
	Specific fuel consumption
	Velocities
	Temperatures
	Densities
	Nozzle areas
	Mass flow
	Fan total pressure ratio
	N1
	N2
	Isentropic fan efficiency
	Maximum turbine entry temperature
Trajectory information	
Time	
Flight position	x, y and z position
Flight angles	Glide slope, roll angle, direction, cruise angle, pitch angle
Velocity	True air speed
	Thrust or N1
Gear deployment	
Extension of high lift devices	Flap angle, slat angle, spoiler extension

B

Ground reflection

B.1. Ground reflection PANAM AzB

For ground reflection calculations in PANAM the following equations are used. All equations originate from reference [17]. The main equation used is given in B.1. This is a correction factor for the noise received by the observer.

$$D_{Z,n}(s,\alpha) = -D_{Z,0,n}(s) \cdot \Delta(\alpha) \tag{B.1}$$

In this equation $D_{Z,0,n}$ is the damping of the n_{th} Octave-band as function of the height with α is zero degrees between the aircraft and the observer. This equation is given in formula B.2. $\Delta(\alpha)$ is calculated using equation B.1.

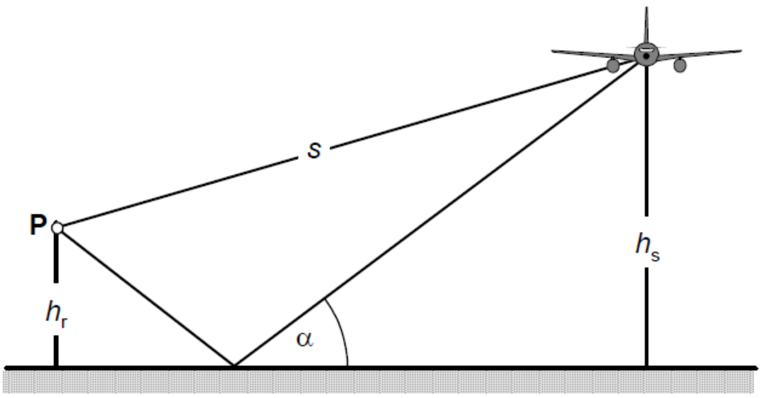

Figure B.1: Ground reflection geometry [17]

$$D_{Z,0,n} = \frac{G_n \cdot s/s_1}{\sqrt{1+(s/s_1)^2}} \tag{B.2}$$

$$\Delta(\alpha) = \begin{cases} 1 - \sin\alpha/\sin 15°, & \text{if } 0 < \alpha < 15° \\ 0, & \text{if } \alpha \leq 0° \text{or } \alpha \geq 15° \end{cases}$$

Where in equation B.2 s is the direct distance between observer and the aircraft. s_1 is the normalisation distance which is 700 m. G_n is obtained out of table B.1.

Table B.1: Ground reflection PANAM [17]

n	Oktavmitten-frequenz (Hz)	d_n (dB)	G_n (dB)
1	63	$0.33 \cdot 10^{-3}$	5
2	125	$0.66 \cdot 10^{-3}$	7.5
3	250	$1.3 \cdot 10^{-3}$	10
4	500	$2.3 \cdot 10^{-3}$	9
5	1000	$4.9 \cdot 10^{-3}$	8
6	2000	$10.2 \cdot 10^{-3}$	7
7	4000	$25.6 \cdot 10^{-3}$	6
8	8000	$43.0 \cdot 10^{-3}$	5

B.2. Ground attenuation correction factor NIROS

The ground attenuation correction factor in NIROS is calculated using B.3.

$$\Lambda(\beta, l) = \tau(l) \cdot \Lambda(\beta) \tag{B.3}$$

where

$$\tau(l) = \begin{cases} 1.089 \cdot [1 - e^{-0.00274 l}], & \text{for } 0 \leq l \leq 914m \\ 1, & \text{for } l > 914m \end{cases}$$

$$\Lambda(\beta) = \begin{cases} 1.137 - 0.0229\beta + 9.72 \cdot e^{-0.142\beta}, & \text{for } 0^\circ \leq \beta \leq 50^\circ \\ 0, & \text{for } 50^\circ \leq \beta \leq 90^\circ \end{cases}$$

C

Routes Schwerin-Parchim airport

This appendix will give the noise prediction results using the ground track out of the AIP database to predict the noise of an A319 approach and landing at Schwerin-Parchim airport.

C.1. BKD2E Approach

Runway 06 at Schwerin-Parchim airport has an elevation of 147 ft, a length of 3000m and a width of 55m. In figure C.2 the altitude, corrected net thrust and velocity of the approaching aircraft are shown.

In figure C.3 the result of the NIROS simulation with BKD2E ground track is given. In the contour the ground track of the aircraft can clearly be distinguished. However the bank angle has almost no influence on the noise when comparing it with the result with a straight ground track.

C.2. BKD5H Departure

The corrected net thrust, velocity and altitude of the NIROS simulation with the BKD5H ground track is given in figure C.5.

In figure C.6 the result of the NIROS simulation with BKD2E ground track is given. In the contour the ground track of the aircraft can clearly be distinguished. However the bank angle has again no influence on the noise when comparing it with the result with a straight ground track.

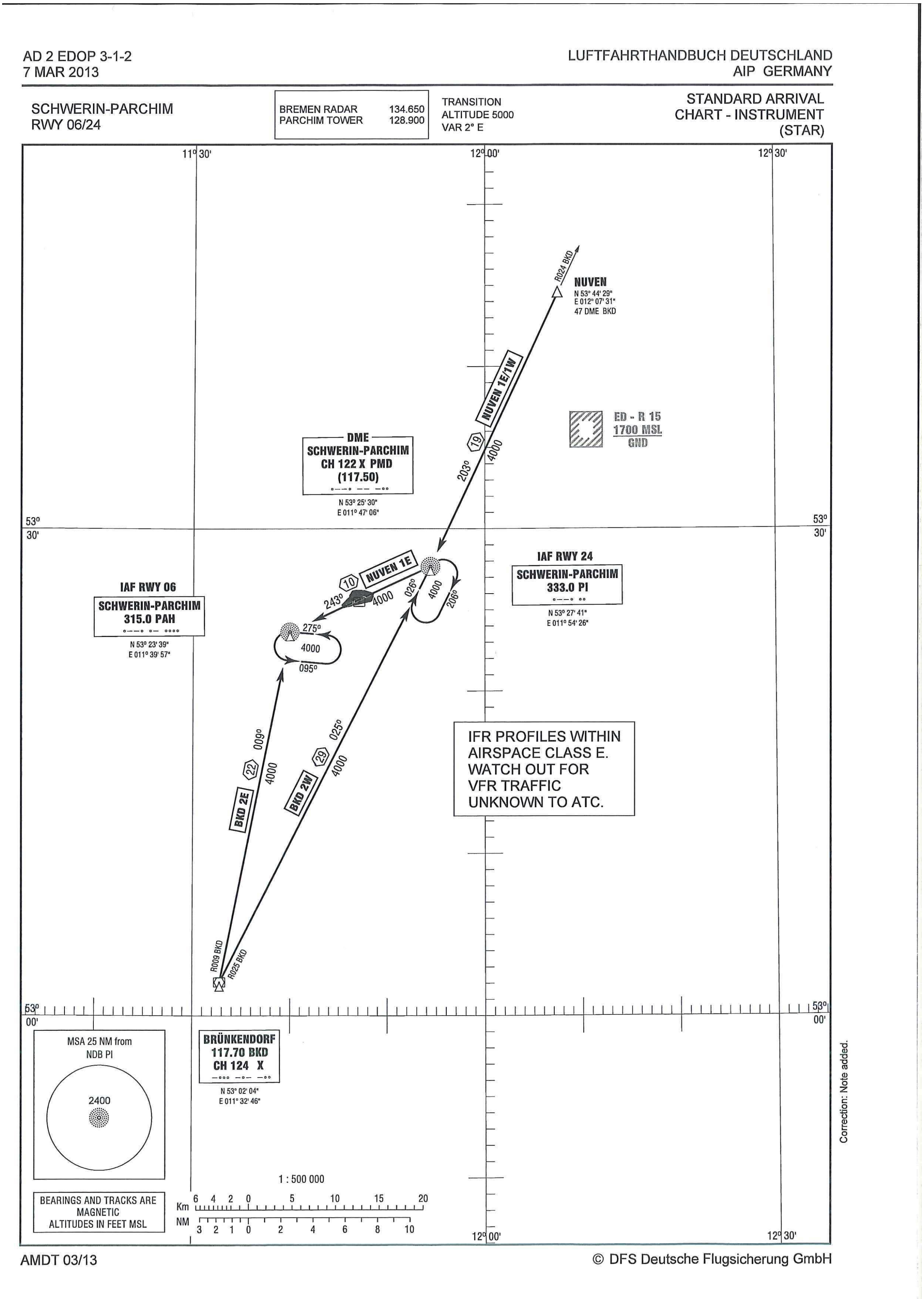

Figure C.1: BKD2E Approach AIP

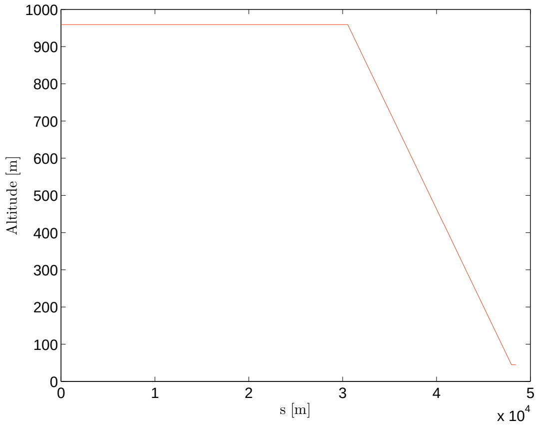

(a) Altitude

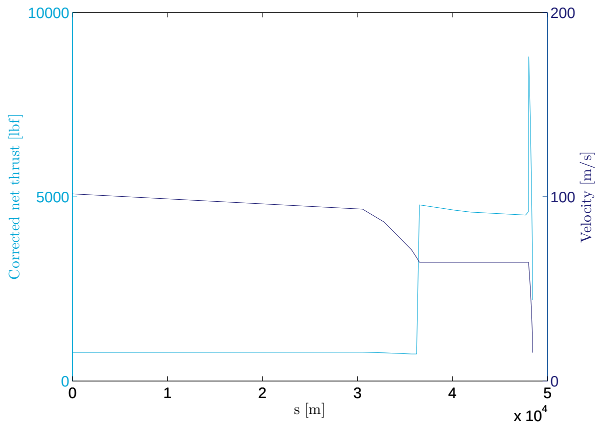

(b) Thrust and velocity

Figure C.2: NIROS STANDARD approach with BKD2E groundtrack

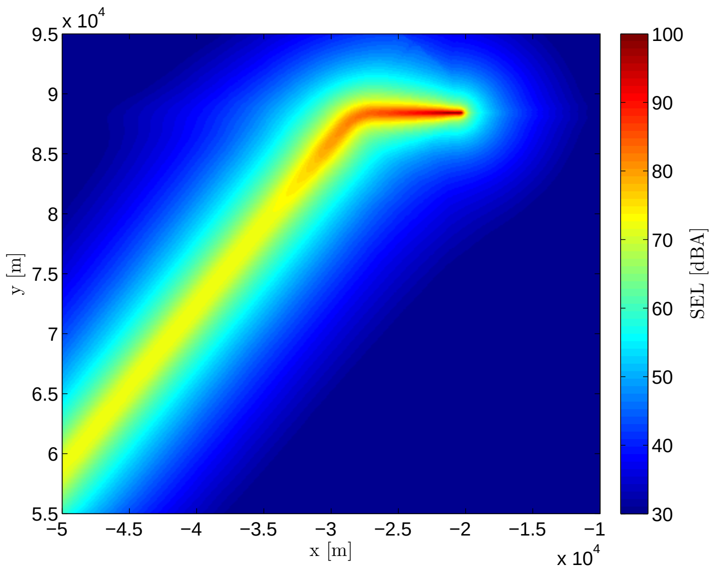

Figure C.3: Noise contours approach NIROS with BKD2E ground track

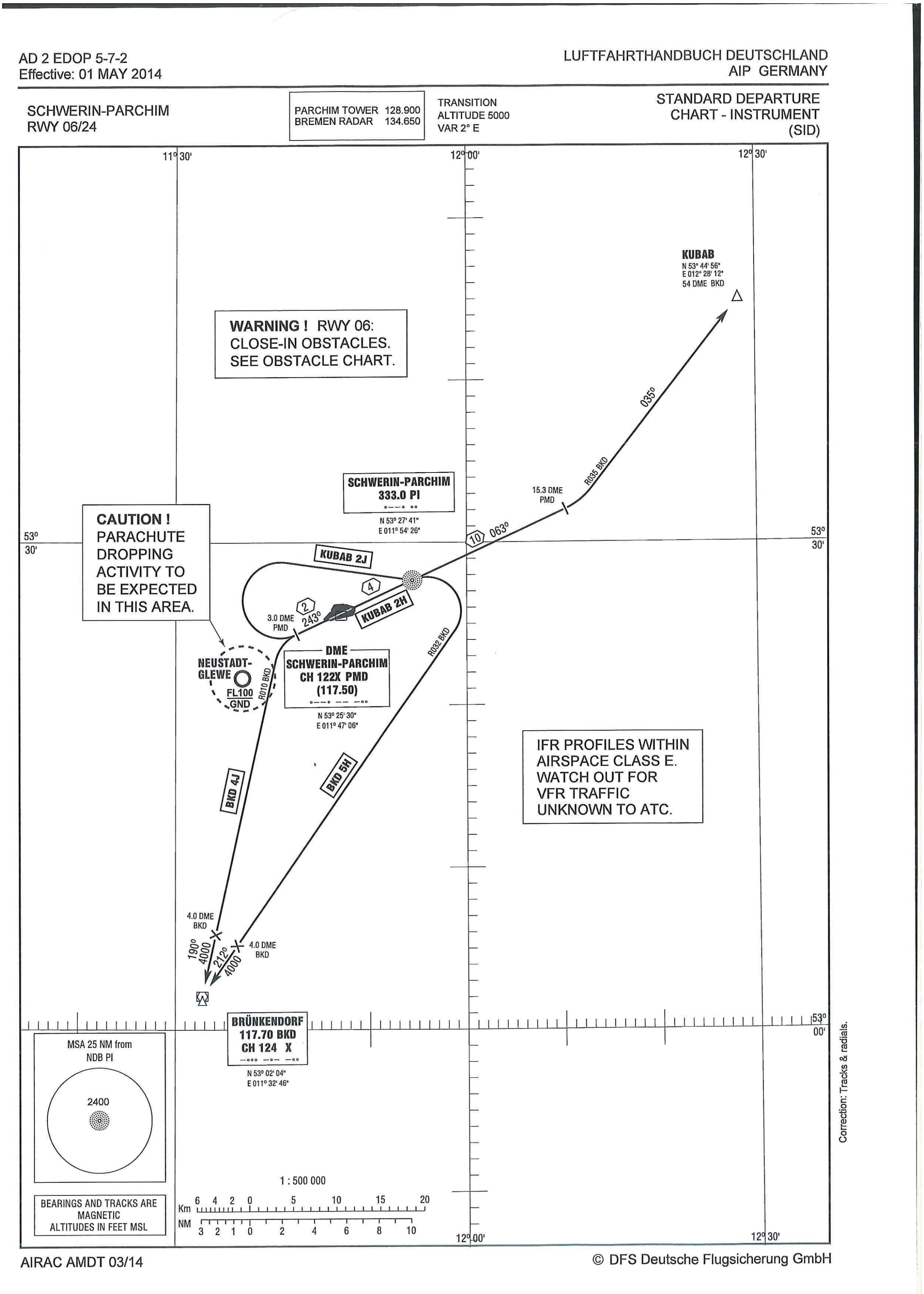

Figure C.4: BKD5H Departure AIP

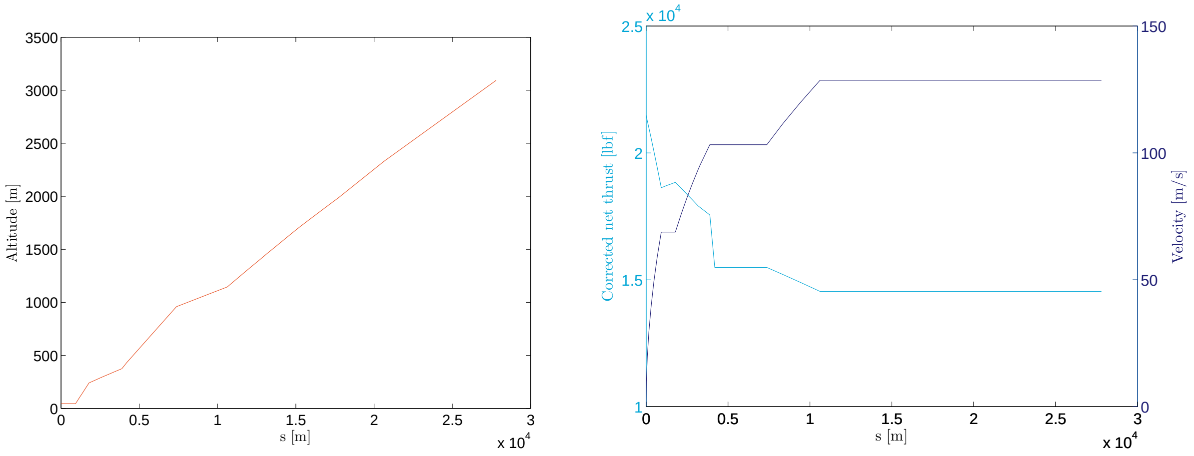

(a) Altitude

(b) Thrust and velocity

Figure C.5: NIROS STANDARD departure with BKD5H groundtrack

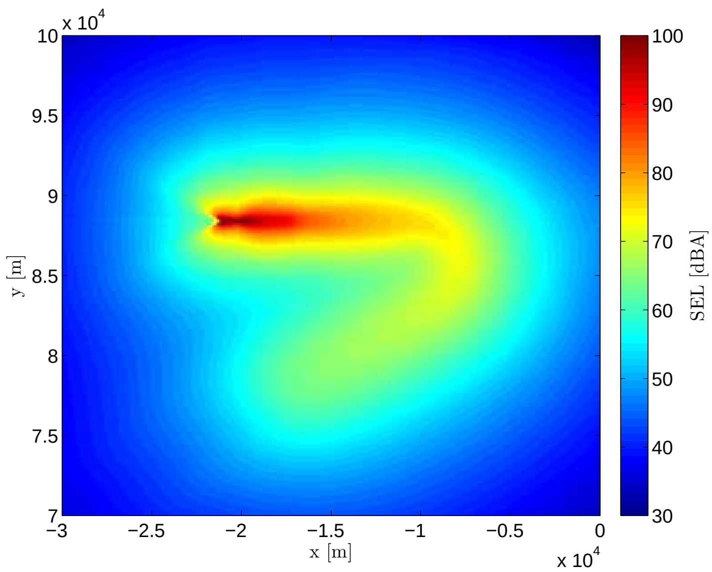

Figure C.6: Noise contour departure NIROS with BKD5H ground track